

A Survey on Generative Diffusion Model

Hanqun Cao, Cheng Tan, Zhangyang Gao, Guangyong Chen, Pheng-Ann Heng, *Senior Member, IEEE*, and Stan Z. Li, *Fellow, IEEE*

Abstract—Deep learning shows excellent potential in generation tasks thanks to deep latent representation. Generative models are classes of models that can generate observations randomly with respect to certain implied parameters. Recently, the diffusion Model has become a raising class of generative models by virtue of its power-generating ability. Nowadays, great achievements have been reached. More applications except for computer vision, speech generation, bioinformatics, and natural language processing are to be explored in this field. However, the diffusion model has its genuine drawback of a slow generation process, leading to many enhanced works. This survey makes a summary of the field of the diffusion model. We first state the main problem with two landmark works – DDPM and DSM. Then, we present a diverse range of advanced techniques to speed up the diffusion models – training schedule, training-free sampling, mixed-modeling, and score & diffusion unification. Regarding existing models, we also provide a benchmark of FID score, IS, and NLL according to specific NFE. Moreover, applications with diffusion models are introduced including computer vision, sequence modeling, audio, and AI for science. Finally, there is a summarization of this field together with limitations & further directions. Github: <https://github.com/chq1155/A-Survey-on-Generative-Diffusion-Model>.

Index Terms—Diffusion Model, advanced improvement on diffusion, diffusion application.



1 INTRODUCTION

How can we empower machines with human-like imagination? Deep generative models, e.g., VAE [1], [2], [3], [4], EBM [5], [6], [7], [8], [9], [10], [11], [12], [13], [14], [15], [16], [17], [18], [19], [20], [21], GAN [22], [23], [24], normalizing flow [25], [26], [27], [28], [29], [30] and diffusion models [31], [32], [33], [34], [35], have shown great potential in creating new patterns that humans cannot properly distinguish. We focus on diffusion-based generative models, which do not require aligning posterior distributions as VAE, dealing with intractable partition functions as EBM, training additional discriminators as GAN, or imposing network constraints as normalizing flow. Thanks to the aforementioned virtues, diffusion-based methods have drawn considerable attention from computer vision, and natural language processing, to graph analysis. However, there is still a lack of systematic taxonomy and analysis of research progress on diffusion models.

Advances in the diffusion model have provided tractable probabilistic parameterization for describing the model, a stable training procedure with sufficient theoretical support, and a unified loss function design with high simplicity. The diffusion model aims to transform the prior data distribution into random noise before revising the transformations

step by step so as to rebuild a brand new sample with the same distribution as the prior [36]. In recent years, the diffusion model has displayed its exquisite potential in the field of computer vision (CV) [31], [37], bioinformatics [38], [39], and speech processing [40], [41]. For instance, denoising diffusion GANs generated high-resolution fake images with just four sampling steps beats GAN [42]. Luo *et al.* [33] firstly generated antibody CDR sequences and structures at the atomic resolution by using DDPMs on protein features. Wavegrad [43] generated high fidelity audio samples with constant steps of generations, outperforming existing GAN-based audio generative models. Inspired by the so-far successes of the diffusion model in CV, bioinformatics, and speech processing domains, applying diffusion models to generation-related tasks of the other domains would be a favorable path for exploiting powerful generative capacity.

On the other hand, the diffusion model has the inherent drawback of plenty of sampling steps and a long sampling time compared to Generative Adversarial Networks (GANs) and Variational Auto-Encoders (VAEs). It is because the diffusion step using the Markov kernel only requires tiny perturbation, which leads to a large number of diffusion. Meanwhile, the tractable model requires the same number of steps during inference. Thus, it takes thousands of steps to sample from a random noise until it eventually alters to high-quality data similar to the prior. Furthermore, other problems such as variation gap optimization and the inability of dimension deduction. Therefore, lots of works aspired to accelerate the diffusion process along with improving sampling quality [47], [48], [49]. For example, DPM-solver takes the advantage of ODE's stability to generate samples of the State-of-the-art within 10 steps [50]. ES-DDPM [51] succeeds in combining trajectory learning together with a variational auto-encoder to achieve high-speed sampling for diffusion models. Partially inspired by Bao *et al.* [50], we summarize improvement works on diffusion models into four classes. (1) training schedule, (2) advanced training-

- H. Cao is with the Department of Math, The Chinese University of Hong Kong, Hong Kong, China, and also with the AI Lab, School of Engineering, Westlake University, Hangzhou, China, and Zhejiang Lab, Hangzhou, China. Email: 1155141481@link.cuhk.edu.hk.
- C. Tan and Z. Gao are with Zhejiang University, Hangzhou, China, and also with the AI Lab, School of Engineering, Westlake University, Hangzhou, China. Email: tancheng, gaozhangyang@westlake.edu.cn.
- G. Chen is with Zhejiang Lab, Hangzhou, China. Email: gy-chen@zhejianglab.com.
- P.-A. Heng is with the Department of Computer Science and Engineering, The Chinese University of Hong Kong, Hong Kong, China.
- Stan Z. Li is with the AI Lab, School of Engineering, Westlake University, Hangzhou, China. Email: Stan.ZQ.Li@westlake.edu.cn.
- H. Cao, C. Tan, and Z. Gao contributed equally to this work.

Manuscript received April 19, 2005; revised August 26, 2015.

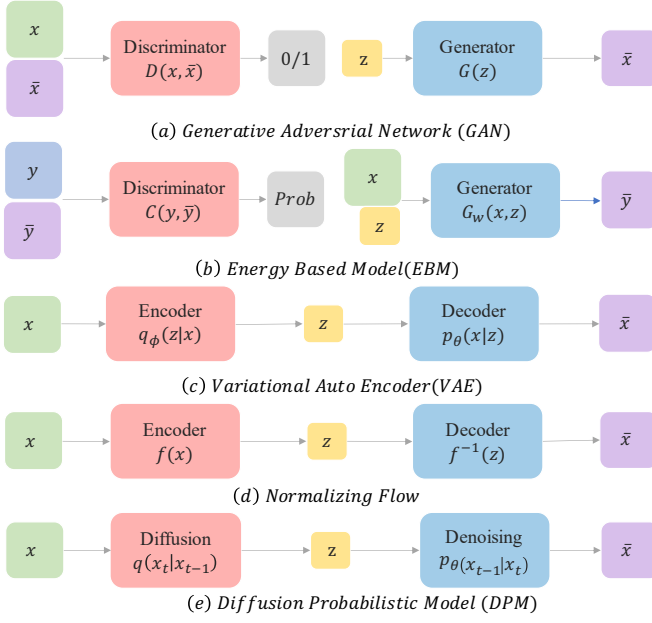


Fig. 1. In this figure, we provide an intuitive mechanism for each class of generative models. **(a)** Generative Adversarial Net (GAN) [44] applies adversarial training strategy onto the generator so that it can generate samples that cannot be distinguished by the real-fake discriminator together with the prior. **(b)** Energy-Based Model (EBM) [45] trains in a similar way that it finds a suitable energy function that consists of a softmax discriminator and a prior-input generator such that it can output the best matching sample for random input. **(c)** Variational Auto-Encoder (VAE) [46] applies the encoder to project the prior into a latent space from which the decoder can sample. **(d)** Normalizing flow (NF) [29] employs a well-designed reversible flow function for turning input into latent variable before returning to samples with the inverse of flow function. **(e)** Diffusion model gradually injects noise into original data until it turns to the known noise distribution before reversing each step in the sampling steps.

free sampling, (3) mixed-generative modeling, and (4) score & diffusion unification. The detailed content is provided in Section 3.

Hence, based on the wide range of applications along with multi-perspective thinking on algorithm improvement, we target at providing a detailed survey about current aspects of diffusion models. By classifying enhanced algorithms and applications on other domains, the core contributions of this review are as follows:

- Summarize essence mathematical formulation and derivation of fundamental algorithms in the field of diffusion model, including method formulation, training strategy, and sampling algorithm.
- Present comprehensive and up-to-date classification of improved diffusion algorithms and divide them into five categories: distillation, noise/trajectory learning, advanced training-free sampling, mixed-generative modeling, and score & diffusion unification.
- Provide extensive statements about the application of diffusion models on computer vision, natural language processing, bioinformatics, and speech processing which include domain-specialized problem formulation, related datasets, evaluation metrics, and downstream tasks, along with sets of benchmarks.

- Clarify current limitations of models and possible further-proof directions concerning the field of diffusion models.

2 PROBLEM STATEMENT

2.1 Notions and Definitions

2.1.1 Discrete or continuous?

There are two main classes of diffusion models – discrete process and continuous process. The discrete process assumes the number of total steps as T for each integer step $t \in [0, T]$. The continuous process assumes the whole process as the time from 0 to 1, where time 0 is the beginning and time 1 is the ending. For either kind of process, there exist similar distribution states and transition kernels. However, the discrete processes can only obtain integer time steps without knowing the gap between non-integer time steps. The continuous process takes the virtue of real-time information, which makes the continuous process obtains better performances.

2.1.2 State

Either type of process has states. States are a set of data distributions that describe the whole process of diffusion models. In the beginning, the noise is injected into the starting distribution, which is called prior state x_0 . With enough steps of noise injection, the distribution finally comes into a known noise distribution (mostly Gaussian), which is called the final state x_T (Discrete)/ x_1 (Continuous). Then, the other distributions between the prior state and the final state are called intermediate states x_t .

2.1.3 Process & Transition Kernel

As mentioned above, the process that transforms the prior to the known noise is defined as the forward/diffusion process F . The process following the opposite direction to the forward process is called reverse/denoised process R . The reverse process samples the noise gradients step by step into the prior state, which is the sample. In either process, the interchange between any two states is achieved by the transition kernel. The most frequently used kernel is the Markov kernel since it ensures the randomness in the forward process and the reverse process.

Forward Process: To present a unified framework, the forward process consists of plenty of forward steps which are the forward transition kernels:

$$F(x, \sigma) = F_T(x_{T-1}, \sigma_T) \cdots \circ F_t(x_{t-1}, \sigma_t) \cdots \circ F_1(x_0, \sigma_1) \quad (1)$$

$$x_t = F_t(x_{t-1}, \sigma_t) \quad (2)$$

Different from the discrete case, for any time $0 \leq t < s \leq 1$, the forward process is defined:

$$F(x, \sigma) = F_{s1}(x_s, \sigma_{s1}) F_{0t} \circ F_{ts}(x_t, \sigma_{ts}) \circ F_{0t}(x_0, \sigma_{0t}) \quad (3)$$

$$x_s = F_{ts}(x_t, \sigma_{ts}) \quad (4)$$

where F_t is the forward transition kernel at time t with the variables intermediate state x_{t-1} & x_{ts} and the noise

scale σ_t & σ_{ts} . The difference between this expression and normalizing flow is the variable noise scale, which controls the randomness of the whole process. When the noise is close to 0, the process will become the normalizing flow which is deterministic.

Reverse Process: Similarly, the reverse process is defined as:

$$R(x, \sigma) = R_1(x_1, \sigma_1) \cdots \circ R_t(x_t, \sigma_t) \cdots \circ R_T(x_T, \sigma_T) \quad (5)$$

$$x_{t-1} = R_t(x_t, \sigma_t) (\text{Discrete}) \quad (6)$$

$$R(x, \sigma) = R_{t0}(x_t, \sigma_{t0}) \cdots \circ R_{st}(x_s, \sigma_{st}) \cdots \circ R_{1s}(x_T, \sigma_{1s}) \quad (7)$$

$$x_t = R_{st}(x_s, \sigma_{st}) (\text{Continuous}) \quad (8)$$

where R_t is the forward transition kernel at time t with the variables intermediate state x_t & x_{st} and the noise scale σ_t & σ_{st} .

Denote the sampled data as \tilde{x}_0 the generalized process can be expressed as:

$$\tilde{x}_0 = R_1(x_1, \sigma_1) \cdots \circ R_t(x_t, \sigma_t) \cdots \circ R_T(x_T, \sigma_T) \circ F_T(x_{T-1}, \sigma_T) \cdots \circ F_t(x_{t-1}, \sigma_t) \cdots \circ F_1(x_0, \sigma_1) \quad (9)$$

$$\tilde{x}_0 = R_{t0}(x_t, \sigma_{t0}) \cdots \circ R_{st}(x_s, \sigma_{st}) \cdots \circ R_{1s}(x_T, \sigma_{1s}) \circ F_{s1}(x_s, \sigma_{s1}) F_{0t} \circ F_{ts}(x_t, \sigma_{ts}) \circ F_{0t}(x_0, \sigma_{0t}) \quad (10)$$

2.1.4 Training Objective

The diffusion model as one type of the generative model follows the same training objective as variational autogressive-encoder and normalizing flow, which is keeping prior distribution x_0 and sample distribution \tilde{x}_0 as close as possible. This is implemented by maximizing the log-likelihood [36]:

$$\mathbb{E}_{F(x_0, \sigma)} [-\log R(x_0, \tilde{\sigma})] \quad (11)$$

where the $\tilde{\sigma}$ in the reverse process differs from the one in the forward process.

2.2 Problem Formulation

Based on the unified framework, two landmark works – DDPM (Discrete) [52] and Score SDE (Continuous) [53] are stated below with customized transition kernels and training objectives.

2.2.1 Diffusion Model Formulation

The original idea of the diffusion probabilistic model is to recreate a specific distribution that starts with random noise. Thus, the distributions of generated samples are required to be as close as the ones of original samples.

Diffusion Forward Process: Given data x_0 , a sequence of latent x_1, x_2, \dots, x_T the same size as x_0 , and a sequence of variance schedule consists of $\beta_1, \beta_2, \dots, \beta_T$. We define the forward process as a sequence of Markov kernels named diffusion/forward step [52]:

$$q(x_t | x_{t-1}) := \mathcal{N}(x_t, \sqrt{1 - \beta_t} x_{t-1}, \sqrt{\beta_t} \mathbf{I}), t \in [1, T] \quad (12)$$

TABLE 1
Notions in Diffusion Systems

Notations	Descriptions
t	Discrete time t on the range of $[0, T]$
z_t	Random noise with normal distribution
\mathcal{N}	Normal distribution
β_t	Variance scale coefficients
$\tilde{\beta}(t)$	Continuous-time β_t
σ_t	Noise scale of perturbation
$\sigma(t)$	Continuous-time σ_t
α_t	$1 - \beta_t$
$\tilde{\alpha}(t)$	Continuous-time α_t
$\tilde{\alpha}_t$	Cumulative product of α_t
$\gamma(t)$	Signal-to-Noise ratio
η_t	Step size of annealed Langevin dynamics
x	Unperturbed data distribution
\tilde{x}	Perturbed data distribution
x_0	Prior distribution of data
x_t	Diffused data at time t
x_t	Partly diffused data at time t
x_T	Random noise after diffusion
$q(\cdot \cdot)$	Diffusion/Forward step
$p(\cdot \cdot)$	Reverse step
$f(\cdot, \cdot)$	Drift coefficient of SDE
$g(\cdot)$	Simplified diffusion coefficient of SDE
$\mathcal{D}(\cdot, \cdot)$	Degrader at time t
$\mathcal{R}(\cdot, \cdot)$	Reconstructor at time t
w, \tilde{w}	Standard Wiener process
$\nabla_x \log p_t(x)$	Score function w.r.t x
$\mu_\theta(x_t, t)$	Mean coefficient of reversed step
$\Sigma_\theta(x_t, t)$	Variance coefficient of reversed step
$\epsilon_\theta(x_t, t)$	Noise prediction model
$s_\theta(x)$	Score network model
L_0, L_{t-1}, L_T	Forward loss, reversed loss, decoder loss
L_{vb}	Evidence Lower Bound
L_{simple}	Simplified denoised diffusion loss
θ	learnable parameters

By a sequence of diffusion steps from x_0 to x_T , We have the Forward/Diffusion Process:

$$q(x_{1:T} | x_0) := \prod_{t=1}^T q(x_t | x_{t-1}), t \in [1, T] \quad (13)$$

Diffusion Reverse Process: Given the forward process above, we define the Reverse step as the inverse step with respect to learned Gaussian transitions parameterized by θ [52]:

$$p_\theta(x_{t-1} | x_t) := \mathcal{N}(x_{t-1}; \mu_\theta(x_t, t), \Sigma_\theta(x_t, t)), t \in [1, T] \quad (14)$$

By a sequence of reverse step from x_T to x_0 , we have the Reverse Process starting at $p(x_T) = \mathcal{N}(x_T; \mathbf{0}, \mathbf{I})$:

$$p_\theta(x_{0:T}) := p(x_T) \prod_{t=1}^T p_\theta(x_{t-1} | x_t), t \in [1, T] \quad (15)$$

Consequently, the distribution $p_\theta(x_0) = \int p_\theta(x_{0:T}) dx_{1:T}$ should be the distribution of x_0 .

Diffusion Training Objective: By minimizing the negative log-likelihood (NLL), the minimization problem can be formulated as:

$$\begin{aligned}
 \mathbb{E}[-\log p_\theta(x_0)] &\leq \mathbb{E}_q \left[-\log \frac{p_\theta(x_{0:T})}{q(x_{1:T} | x_0)} \right] \\
 &= \mathbb{E}_q \left[-\log p(x_T) - \sum_{t \geq 1} \log \frac{p_\theta(x_{t-1} | x_t)}{q(x_t | x_{t-1})} \right] \\
 &= \mathbb{E}_q \left[\underbrace{D_{\text{KL}}(q(x_T | x_0) \| p(x_T))}_{L_T} \right. \\
 &\quad \left. + \sum_{t \geq 1} \underbrace{D_{\text{KL}}(q(x_{t-1} | x_t, x_0) \| p_\theta(x_{t-1} | x_t))}_{L_{t-1}} \right. \\
 &\quad \left. - \underbrace{\log p_\theta(x_0 | x_1)}_{L_0} \right] \\
 &=: L
 \end{aligned} \tag{16}$$

Here we use the symbol of Ho *et al.* [52]. Denote L_T as the forward loss, which represents the divergence between the forwarding process and the distribution of random noise. By equation (2), we can learn that L_T is a constant depending on variance schedule β_1, \dots, β_T ; Denote L_0 as the decode loss; Besides, denote $L_{1:T-1}$ as the reverse loss, which is the sum of divergence between posterior of forwarding step and reverses step at each step.

As for the continuous case in Score SDE proposed by Song *et al.*, denoised diffusion process with the discrete perturbation kernels $p_{\alpha_t}(x|x_0)$ can be transformed as:

$$dx = -\frac{1}{2}\beta(t)x dt + \sqrt{\beta(t)}dw \tag{17}$$

where $\beta(t)$ is the continuous-time variable of variance schedule β_t . Besides, this kind of SDE is called Variation Preserving (VP) SDE.

Signal-to-Noise Ratio: The Signal-to-Noise Ratio is defined with mean coefficients and variance coefficients at time t as:

$$\gamma(t) := \frac{\alpha_t^2}{\sigma_t^2}, t \in [0, 1] \tag{18}$$

The Signal-to-Noise Ratio proposed by Kingma *et al.* [54] is a decreasing function that is utilized as a variable in re-expressing the training objective to simplify and unify the training objective of different types of models.

2.2.2 Score Matching Formulation

The main idea of score matching is to train a score network x_θ to predict the score of a specific data distribution [55], [56], which is defined as $\nabla_x \log p_{data}(x)$ by means of perturbing data with different noise schedules. The score matching process is defined as:

Forward Score SDE Process: In Song *et al.* [53], Diffusion Process can be viewed as a continuous case described by Stochastic Differential Equation, and it is equal to the solution to Itô SDE [57]:

$$dx = f(x, t)dt + g(t)dw, t \in [0, T] \tag{19}$$

where w is the standard Wiener process/Brownian Motion, $f(\cdot, t)$ is the drift coefficient of $x(t)$, and $g(\cdot)$ is the

simplified version of diffusion coefficient of $x(t)$, which is assumed not dependent on x . Besides, $p_0, p_t(x)$ denote the data distribution and probability density of $x(t)$. p_T denotes the original prior distribution which gains no information from p_0 . When the coefficients are piece-wise continuous, the forward SDE equation admits a unique solution [58].

Similar to the discrete case, the forward transition in the SDE framework is derived as (we follow the symbol provided by Watson *et al.* [59])

$$\begin{aligned}
 q(x_t | x_s) &= \mathcal{N}\left(x_t | f_{ts}x_s, g_{ts}^2 I\right), 0 < s < t \leq 1 \\
 q(x_s | x_t, x_0) &= \mathcal{N}\left(x_s | \frac{1}{g_{t0}^2} \left(f_{s0}g_{ts}^2 x_0 + f_{ts}g_{s0}^2 x_t\right), \frac{g_{s0}^2 g_{ts}^2}{g_{t0}^2} I\right)
 \end{aligned} \tag{20}$$

where $f_{ts} = \frac{f(t)}{f(s)}$ and $g_{ts} = \sqrt{g(t)^2 - f_{ts}^2 g(s)^2}$.

Reversed Score SDE Process: In contrast to the Forward SDE Process, the Reversed SDE Process is defined with respect to the reverse-time Stochastic Differential Equation by running backward in time [53]:

$$dx = [f(x, t) - g(t)^2 \nabla_x \log p_t(x)] dt + g(t)d\bar{w}, t \in [0, T] \tag{21}$$

where \bar{w} is known as the standard Wiener Process from T to 0 , and t is defined to be infinitesimal negative timestep. Furthermore, $\nabla_x \log p_t(x)$ is the score to be matched [60].

$$L := \frac{1}{2} \mathbb{E}_q [\|s_\theta - \nabla_x \log p_{data}(x)\|_2^2] \tag{22}$$

Song *et al.* has proposed denoising score matching and sliced score matching [61] to avoid extra computation due to higher-order gradients.

$$L := \frac{1}{2} \mathbb{E}_{q_{\sigma((\tilde{x}|x)p_{data}(x))}} [\|s_\theta(\tilde{x}) - \nabla_{\tilde{x}} \log q_{\sigma}(\tilde{x}|x)\|_2^2] \tag{23}$$

$$\mathbb{E}_{p_v} \mathbb{E}_{p_{data}} \left[v^\top \nabla_x s_\theta(x) v + \frac{1}{2} \|s_\theta(x)\|_2^2 \right] \tag{24}$$

However, because of the low-manifold problem in real data as well as the sampling problem in the low-density region, denoised score matching could be the better solution for improving score matching.

As for the continuous case in Score SDE proposed by Song *et al.*, denoised score matching with N noise scales can be derived as

$$dx = \sqrt{\frac{d[\sigma^2(t)]}{dt}} dW \tag{25}$$

where $\sigma(t)$ is the continuous-time variable of discrete noise scale σ_t . Moreover, this kind of SDE is called Variation Explosion (VE) SDE.

Indeed, score matching and denoising diffusion are the same kinds of processes. To some extent, every perturbation of the scoring network can be seen as the accumulated transformation of previous Markov steps. The diffusion process consists of a number of Markov chains,

transforming prior data into random noise. The score network adds a sequence of noises of different scales separately. The smallest scale of noise has no influence on data distribution, the largest scale of noise turns the data into random noise. From the perspective of the training objective, the training scheme of DDPM is actually score matching. By DDPM's training strategy introduced below, minimizing L_{simple} is equivalent to estimating the gradient of the posterior, which can be viewed as one kind of score.

2.2.3 Probability Flow ODE Formulation

Probability Flow ODE (Diffusion ODE) is the continuous-time differential equation proposed by Song *et al.* [53]. Inspired by Maoutsa *et al.* [62] and Chen *et al.* [63], general case SDE can be derived into a special form of ODE. In the case that functions G is independent of x , the probability flow ODE is

$$dx = \{f(x, t) - \frac{1}{2}G(t)G(t)^T \nabla_x \log p_t(x)\} dt \quad (26)$$

Probability flow ODE supports the deterministic process which shares the same marginal probability density. In contrast to SDE, probability flow ODE can be solved with larger step sizes as they have no randomness. Due to advantages of ODE, several works such as PNDMs [64] and DPM-Solver [50] obtain amazing results by modeling the diffusion problem as an ODE.

2.3 Training Strategy

2.3.1 Denoising Diffusion Training Strategy

In order to minimize the negative log-likelihood, the only item we can be used to train is $L_{1:T-1}$. By parameterizing the posterior $q(x_{t-1}|x_t, x_0)$ using Baye's rule, we have:

$$q(x_{t-1} | x_t, x_0) = \mathcal{N}(x_{t-1}; \tilde{\mu}_t(x_t, x_0), \tilde{\beta}_t I) \quad (27)$$

where α_t is defined as $1 - \beta_t$, $\bar{\alpha}_t$ is defined as $\prod_{k=1}^t \alpha_k$. Mean and variance schedules can be expressed as:

$$\begin{aligned} \tilde{\mu}_t(x_t, x_0) &:= \frac{\sqrt{\alpha_{t-1}}\beta_t}{1 - \bar{\alpha}_t} x_0 + \frac{\sqrt{\alpha_t}(1 - \bar{\alpha}_{t-1})}{1 - \bar{\alpha}_t} x_t \\ \tilde{\beta}_t &:= \frac{1 - \bar{\alpha}_{t-1}}{1 - \bar{\alpha}_t} \beta_t \end{aligned} \quad (28)$$

Keeping above parameterization as well as reparameterizing x_t as $x_t(x_0, \sigma)$, L_{t-1} can be regarded as an expectation of L2-loss between two mean coefficients:

$$L_{t-1} = \mathbb{E}_q \left[\frac{1}{2\sigma_t^2} \left\| \tilde{\mu}_t(x_t, x_0) - \mu_\theta(x_t, t) \right\|^2 \right] + C \quad (29)$$

Simplifying L_{t-1} by reparameterizing μ_θ w.r.t ϵ_θ , we obtain the simplified training objective named L_{simple} :

$$L_{simple} := \mathbb{E}_{x_0, \epsilon} \left[\frac{\beta_t^2}{2\sigma_t^2 \alpha_t (1 - \bar{\alpha}_t)} \left\| \epsilon - \epsilon_\theta(\sqrt{\bar{\alpha}_t} x_0 + \sqrt{1 - \bar{\alpha}_t} \epsilon) \right\|^2 \right] \quad (30)$$

Most diffusion models until now use the training strategy of DDPMs. But there exist some exceptions. DDIM's training objective can be transformed by adding a constant from DDPM's although it is independent of Markovian step assumption; Training pattern of Improved DDPM named as

L_{hybrid} is to combine training object of DDPM L_{simple} and a term with variational lower bound L_{vlb} . However, L_{simple} still takes the main effect of these training methods.

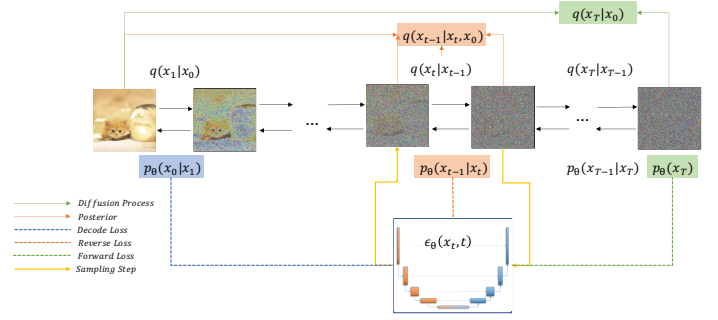


Fig. 2. Pipeline of Denoised Diffusion Probabilistic Model. The arrows pointing from left to right indicate the diffusion process and the arrows pointing in the reverse direction indicate the reverse process. The colored background transition terms are components of ELBO: the blue part stands for decode loss L_0 , the green part represents forward loss L_T , and the orange part constitutes the reverse loss L_T . Dashed lines with different colors show the training pattern of the noise prediction model ϵ_θ . Besides, in any step $1 \leq t \leq T$, the yellow lines denote the ancestral sampling process.

2.3.2 Denoising Score Matching Training Strategy

According to Song *et al.*, the noise distribution is defined to be $q_\sigma(\tilde{x}|x) = \mathcal{N}(\tilde{x}|x, \sigma^2 I)$. Thus, for each given σ , the denoising score matching objective is

$$L(\theta; \sigma) := \frac{1}{2} \mathbb{E}_{p_{\text{data}}(x)} \mathbb{E}_{\tilde{x} \sim \mathcal{N}(x, \sigma^2 I)} \left[\left\| s_\theta(\tilde{x}, \sigma) + \frac{\tilde{x} - x}{\sigma^2} \right\|^2 \right] \quad (31)$$

In the framework of a stochastic differential equation, denoising score matching follows a similar way to discrete case, which is

$$L := \mathbb{E}_t \{ \lambda(t) \mathbb{E}_{x(0)} \mathbb{E}_{x(t)|x(0)} \left[\| s_\theta(x(t), t) - \nabla_{x(t)} \log p(x(t)|x(0)) \|^2 \right] \} \quad (32)$$

where $x(t), x(0)$ are corresponding continuous time variables of x_t, x_0 .

2.4 Sampling Algorithm

Reconstructing data distribution needs sampling. In each sampling step, the sample generated from random noise will be refined again to get closer to the original distribution. However, it takes too many steps to sample with diffusion models, causing a very time-consuming situation. Here we state the two most classic sampling algorithms in the field of diffusion models.

2.4.1 Ancestral Sampling

The initial idea of ancestral sampling is reconstructed with the gradient step by step. At each sampling step, DDPM aims to rebuild the data by inverse Markovian, which is $p(x_{t-1}|x_t)$. Thus, at time t , x_{t-1} is sampled from x_t by

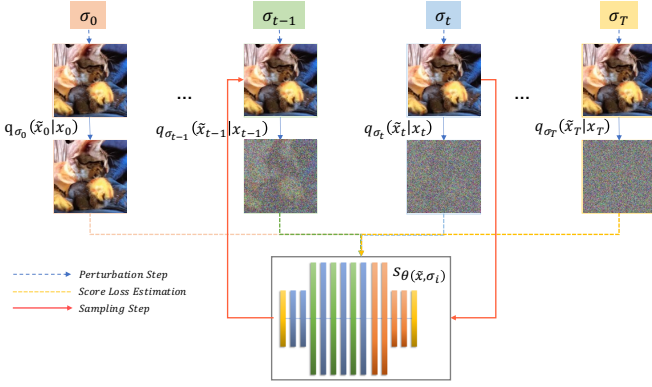


Fig. 3. Pipeline of Denoised Score Matching (DSM). The σ 's in different time states on the top represent alternative scales of noise. The transition states $p_{\sigma_t}(\tilde{x}_t | x_t)$ are the output gradients of the perturbation. Dashed lines with different colors reveal that the scoring network s_θ is trained by minimizing the sum of L2-loss between the output gradient and the score in each noise scale. Besides, in any noise state $1 \leq t \leq T$, the red lines denote the Langevin Dynamics sampling process.

Algorithm 1 Ancestral Sampling

```

 $x_T \sim \mathcal{N}(0, I)$ 
for  $t = T, \dots, 1$  do
  if  $t > 1$  then
     $z \sim \mathcal{N}(0, I)$ 
  else
     $F = 0$ 
  end if
   $x_{t-1} = \frac{1}{\sqrt{\alpha_t}} \left( x_t - \frac{1-\alpha_t}{\sqrt{1-\alpha_t}} \epsilon_\theta(x_t, t) \right) + \sigma_t z$ 
end for
return  $x_0$ 
    
```

2.4.2 Langevin Dynamics Sampling

Langevin dynamics can produce samples from a probability density $p(x)$ with only the score function (Song *et al.*) $\nabla_x \log p(x)$. With a fixed step size $\epsilon > 0$, the recursive method is

$$\tilde{x}_t = \tilde{x}_{t-1} + \frac{\epsilon}{2} \nabla_x \log p(\tilde{x}_{t-1}) + \sqrt{\epsilon} z_t, t \in [1, T] \quad (33)$$

where z_t fits random distribution, and \tilde{x}_0 is the starting point of sampling. In denoised score matching, we aim to train score network s_θ as close as the score function $\nabla_x \log p(x)$. Thus, the annealed Langevin dynamics is

$$\tilde{x}_t = \tilde{x}_{t-1} + \frac{\eta_i}{2} s_\theta(\tilde{x}_{t-1}, \sigma_i) + \sqrt{\alpha_i} z_t \quad (34)$$

where step size η_i is adjusted w.r.t $\epsilon \cdot \frac{\sigma_i^2}{\sigma_L^2}$ to dynamically accelerate the sampling process and perform better sampling quality.

2.4.3 Predictor-corrector (PC) Sampling

PC sampling [65] is inspired by a type of ODE black-box ODE solver [66], [67], [68] in order to produce high-quality samples and trade-off accuracy for efficiency for all reversed SDE. The sampling procedure is made up of a predictor sampler and a corrector sampler. For solving VE SDE and VP SDE, Song *et al.*, [53] used reverse diffusion SDE solver as the predictor, and annealed Langevin dynamics as the corrector.

Algorithm 2 Predictor-Corrector Sampling(VE SDE)

```

 $x_N \sim \mathcal{N}(0, \sigma_{\max}^2 I)$ 
for  $i = N - 1$  to  $0$  do
   $x'_i \leftarrow x_{i+1} + (\sigma_{i+1}^2 - \sigma_i^2) s_\theta * (x_{i+1}, \sigma_{i+1})$ 
   $Z \sim \mathcal{N}(0, I)$ 
   $x_i \leftarrow x'_i + \sqrt{\sigma_{i+1}^2 - \sigma_i^2} Z$ 
  for  $j = 1$  to  $M$  do
     $Z \sim \mathcal{N}(0, I)$ 
     $x_i \leftarrow x_i + \epsilon_i s_\theta * (x_i, \sigma_i) + \sqrt{2\epsilon_i} Z$ 
  end for
end for
return  $x_0$ 
    
```

Algorithm 3 Predictor-Corrector Sampling(VP SDE)

```

 $x_N \sim \mathcal{N}(0, I)$ 
for  $i = N - 1$  to  $0$  do
   $x'_i \leftarrow (2 - \sqrt{1 - \beta_{i+1}}) x_{i+1} + \beta_{i+1} s_\theta * (x_{i+1}, i + 1)$ 
   $z \sim \mathcal{N}(0, I)$ 
   $x_i \leftarrow x'_i + \sqrt{\beta_{i+1}} z$ 
  for  $j = 1$  to  $M$  do
     $Z \sim \mathcal{N}(0, I)$ 
     $x_i \leftarrow x_i + \epsilon_i s_\theta * (x_i, \sigma_i) + \sqrt{2\epsilon_i} Z$ 
  end for
end for
return  $x_0$ 
    
```

2.5 Evaluation Metric

In order to evaluate the properties of generated samples, Evaluation metrics are designed to test the sample quality and diversity.

2.5.1 Inception Score (IS)

The inception score is built with the goal of valuing both the diversity and resolution of generated images based on ImageNet dataset. [69], [70] It can be divided into two parts: diversity measurement and quality measurement. Diversity measurement denoted by p_{IS} is calculated w.r.t. the class entropy of generated samples: the larger the entropy is, the more diverse the samples will be. Quality measurement denoted by q_{IS} is computed through the similarity between a sample and the related class images using entropy. It is because the samples will enjoy high resolution if they are closer to the specific class of images in the ImageNet dataset. Thus, to lower q_{IS} and higher p_{IS} , the KL divergence [71] is applied to inception score calculation:

$$\begin{aligned}
 IS &= D_{KL}(p_{IS} \parallel q_{IS}) \\
 &= \mathbb{E}_{x \sim p_{IS}} \left[\log \frac{p_{IS}}{q_{IS}} \right] \\
 &= \mathbb{E}_{x \sim p_{IS}} [\log(p_{IS}) - \log(q_{IS})]
 \end{aligned} \quad (35)$$

2.5.2 Frechet Inception Distance (FID)

Although there are reasonable evaluation techniques in the Inception Score, the establishment is based on a specific dataset with 1000 classes as well as a trained network that consists of randomness such as initial weights, and code framework. [72] Thus, the bias between ImageNet and real world image may cause an inaccurate outcome. Furthermore,

the number of sample batches is much less than 1000 classes, leading to low-belief statistics.

FID is proposed to solve the bias from specific reference datasets. The score shows the distance between real-world data distribution and the generated samples using the mean and the covariance. [73]

$$\text{FID} = \|\mu_r - \mu_g\|^2 + \text{Tr} \left(\Sigma_r + \Sigma_g - 2(\Sigma_r \Sigma_g)^{1/2} \right) \quad (36)$$

where μ_g, Σ_g are the mean and covariance of generated samples, and μ_r, Σ_r are the mean and covariance of real-world data.

2.5.3 Negative Log Likelihood (NLL)

According to Razavi *et al.*, [74] negative log-likelihood is seen as a common evaluation metric that describes all modes of data distribution. Lots of works on normalizing flow field [75], [76], [77], [78], [79] and VAE field [80], [81], [82] uses NLL as one of the choices for evaluation. Some diffusion models like improved DDPM [47] regard the NLL as the training objective.

$$\text{NLL} = \mathbb{E} \left[-\log p_\theta(x) \right] \quad (37)$$

3 ALGORITHM IMPROVEMENT

Nowadays, the main concern of the diffusion model is to speed up its speed and reduce the cost of computing. With the aid of strong conditioned settings, sampling of diffusion can be achieved in just few steps [48], such as text-to-speech [83], and image super-resolution [84]. In general cases, it takes thousands of steps for diffusion models to generate a high-quality sample. Mainly focusing on improving sampling speed, many works from different aspects come into reality. Besides, other problems such as variational gap optimization, distribution diversification, and dimension reduction are also attracting extensive research interests. In this section, we divide the improved algorithm w.r.t. problems to be solved. For each problem, we present the significance and related detailed classification of solutions (which are shown in Table 2).

3.1 Speed-up Improvement

3.1.1 Training Schedule

The improvement in the training schedule means changing traditional ways of training such as diffusion schemes, noise schemes, and data distribution schemes, which are independent of sampling. Recent related studies have shown the key factors in training schemes that influence learning patterns and models' performance. Thus, in this sub-section, we divide the training enhancement into four categories: knowledge distillation, diffusion scheme learning, noise scale designing, and data distribution replacement.

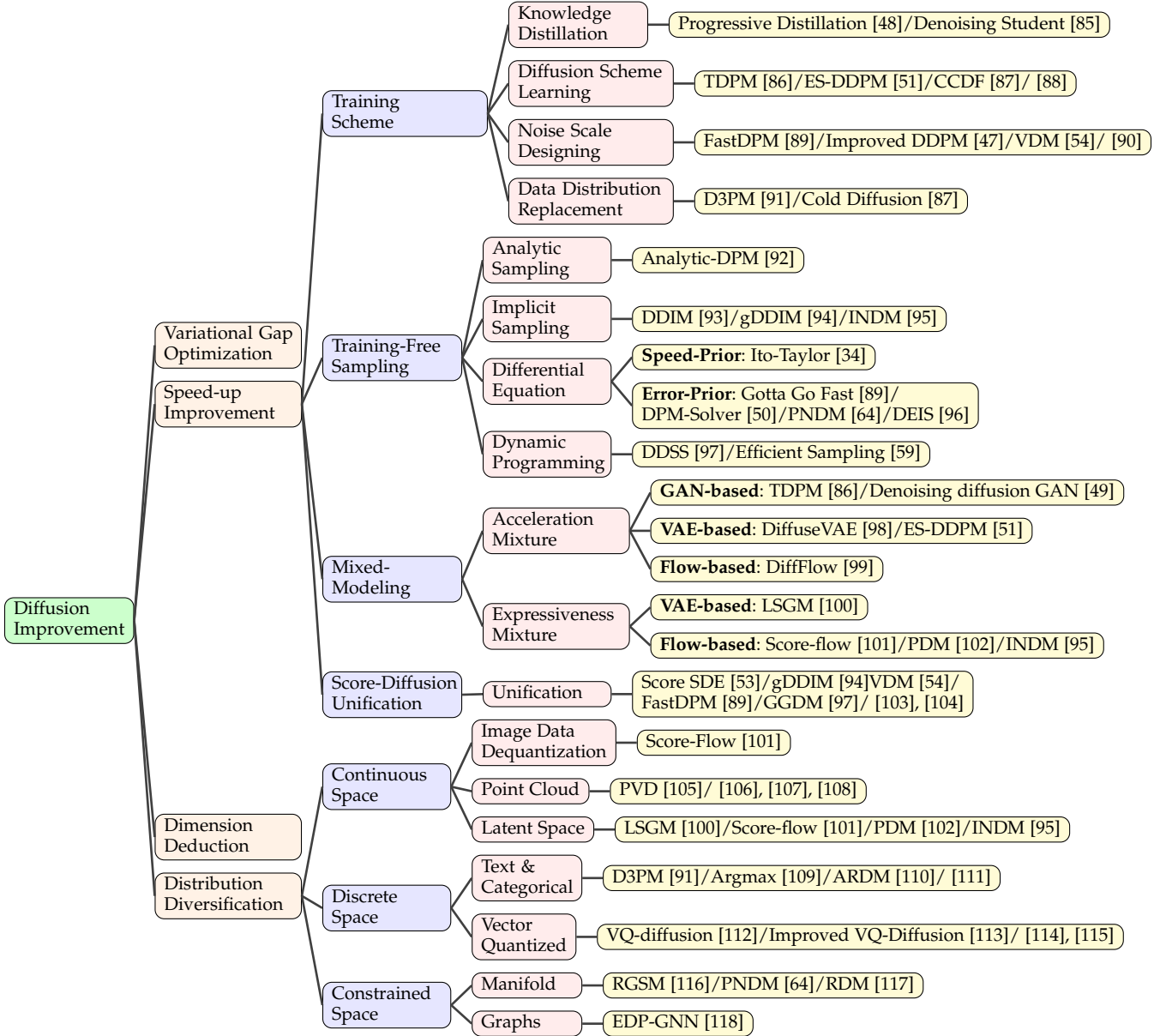
Knowledge Distillation Knowledge distillation is an emerging method for obtaining efficient small-scale networks by transferring "knowledge" from complex teacher models with high learning capacity to simple student models [119]. Thus, student models equip the advantages in model compression and model acceleration.

Salimans *et al.* [48] firstly utilize the core idea into diffusion model improvement by progressively distilling knowledge from one sampling model to another. In each distillation step, student models re-weight from teacher models before being trained to generate one-step samples as close as teacher models do. As a result, student models can halve their sampling steps during each distillation process. Following the same training objective as DDPMs with alternative parameterization methods, the Progressive Distillation model achieved an FID of 2.57 in only 4 steps. This core idea was used in ProDiff [120] in the domain of Text-to-Speech generation. The sampling quality of ProDiff is around the SOTA with only 2 sampling steps, compared with the former SOTA DiffSpeech which needs 128 steps for sampling. Further improvement along the path of distillation includes denoising students, in which the teacher models directly guide the sampling pattern of the student model by minimizing the L2-loss [121] of samples from both models. Denoising students got one-step sampling with an FID score of 9.36, compared with 9.12 for Progressive Distillation one-step generation.

Diffusion Scheme Learning Diffusion scheme learning aims at probing the effect of different diffusion patterns on the model's speed. Recent studies focus on the diffusion steps. TDPM [86] has firstly proposed that truncating both the diffusion process and sampling process leading to less sampling time is beneficial for reducing sampling time along with improving generating quality. The key idea of truncating patterns is generating less diffused data with the help of other generative models like GAN and VAE. TDPM used GAN as well as conditional transport [122] to learn the implicit generative distribution from random noise. Unlike TDPM, Early Stop (ES) DDPM [51] generated implicit distribution by means of generating prior data with VAE which learned the latent space from x_0 . To be more general, CCDF [87] has shown that there exists an optimal step less than T minimizing the estimation error by contraction theory. Besides the Shortcut thinking of reducing steps, Franzese *et al.*, [88] defined the number of training steps as a variable to train the model with more flexibility together with probing the optimal steps.

Noise Scale Designing Different from DDPM which defines noise scale as a constant, exploring works concerning the effect of noise scale learning has also drawn much attention since noise schedule learning also counts during diffusion and sampling. Each sampling step can be seen as a random walk on the direct line pointing to the prior distribution, which shows that noise adjustment may benefit the sampling procedure. Improved DDPM [47] first took noise scale tuning into consideration by way of defining adding a λ -scaled term L_{v1b} on L_{simple} . Different from Improved DDPM, San Roman *et al.*, [90] has proposed a noise estimation method containing another noise prediction network P_θ to update the noise scale in each step before conducting ancestral sampling. Thus, optimizing the loss L_{hybrid} leads to learning the noise schedule. Thankfully, Improved DDPM exceeded DDIM [93] over 50 steps. Furthermore, FastDPM [89] and VDM [54] reparameterized the noise scalar α_t and β_t to directly express the loss term with respect to noise scale

TABLE 2
Classification of Improved Techniques



to optimize the procedure w.r.t noise schedule. To sum up, noise learning guides the random walk of random noise in both the diffusion and sampling processes, leading to more efficient reconstruction.

Data Distribution Replacement Data distribution learning mainly concentrates on processing different types of data distribution. From the perspective of the prior distribution, D3PM [91] promoted diffusion algorithm onto discrete space to deal with discrete data like sentences and images by means of defining

$$q(x_t | x_{t-1}) = \text{Cat}(x_t; p = x_{t-1} \mathbf{Q}_t) \quad (38)$$

where $[\mathbf{Q}_t]_{ij} = q(x_t = j | x_{t-1} = i)$ is defined as the transition, and $\text{Cat}(\cdot)$ is defined as the categorical distribution over the one-hot row vector.

Besides, in order to process multi-nominal discrete data as well as promote better predictions of the data x_0 at each time step, the parameterization and training objectives are:

$$p_\theta(x_{t-1} | x_t) \propto \sum_{\tilde{x}_0} q(x_{t-1}, x_t | \tilde{x}_0) \tilde{p}_\theta(\tilde{x}_0 | x_t) \quad (39)$$

$$L_\lambda = L_{\text{vb}} + \lambda \mathbb{E}_{q(x_0)} \mathbb{E}_{q(x_t|x_0)} [-\log \tilde{p}_\theta(x_0 | x_t)] \quad (40)$$

Furthermore, cold diffusion [87] has shown that data distribution of noise can be set as any distribution by cold diffusion improved sampling to eliminate the prediction error by the wrong design of Reconstructor \mathcal{R} (Generalized term of all types of the samplers). The cold diffusion improved sampling is :

Algorithm 4 Cold Diffusion Sampling

Input: A degraded sample x_t
for $s = t, t - 1, \dots, 1$ **do**
 $\hat{x}_0 \leftarrow R(x_s, s)$
 $x_{s-1} = x_s - D(\hat{x}_0, s) + D(\hat{x}_0, s - 1)$
end for
return x_0

3.1.2 Training-Free Sampling

Many methods are focusing on changing the pattern of training and noise schedule to improve sampling speed, but re-training models cost more computing and lead to the risk of unstable training. Thankfully, there exists a class of methods that directly enhance the sampling algorithm with a pre-trained model which is called training-free sampling. The goal of advanced training-free sampling is to propose an efficient sampling algorithm for acquiring knowledge from the pre-trained models with fewer steps and higher accuracy. It contains four categories: analytical methods, implicit sampler, differential equation solver sampler, and dynamic programming adjustment.

Analytical Method Bao *et al.* firstly propose analytical method named analytic-DPM [92]. It improves DDIM [93] by optimizing the reverse variance by means of KL-Divergence analysis.

Implicit Sampler As mentioned above, it usually takes the same number of steps for the generative process as the diffusion process to rebuild the original data distribution in DDPM. However, the diffusion model has the so-called decoupling property that does not require the equivalent number of steps for diffusing and sampling. Inspired by generative implicit model [123], Song *et al.*, [93] has proposed implicit sampling method equipped with deterministic diffusion and jump-step sampling. Surprisingly, implicit models have no requirement for re-training models since the forward diffusion probabilistic density is kept the same for any time $t \in [0, T]$. DDIM solves the jump-step acceleration using continuous process formulation [63], [124] with the aid of neural ODE as:

$$d\bar{x}(t) = \epsilon_\theta^{(t)} \left(\frac{\bar{x}(t)}{\sqrt{\sigma^2 + 1}} \right) d\sigma(t) \quad (41)$$

where σ_t is parameterized by $\sqrt{1 - \alpha}/\sqrt{\alpha}$, and \bar{x} is parameterized as $x/\sqrt{\alpha}$. Besides, the probability can be treated as one kind of Score SDE, which is derived from the discrete formulation:

$$\frac{x_{t-\Delta t}}{\sqrt{\alpha_{t-\Delta t}}} = \frac{x_t}{\sqrt{\alpha_t}} + \left(\sqrt{\frac{1 - \alpha_{t-\Delta t}}{\alpha_{t-\Delta t}}} - \sqrt{\frac{1 - \alpha_t}{\alpha_t}} \right) \epsilon_\theta^{(t)}(x_t) \quad (42)$$

Based on DDIM, gDDIM [94] generalized implicit diffusion with diverse types of kernels in the SDE framework including DDPM, DDIM, and critically-damped Langevin diffusion (CLD) [125] into a family of DDIM, achieving the acceleration of implicit diffusion model by corresponding ODE and SDE solvers. Different from above, INDM [95] achieves an implicit mechanism by transforming the

nonlinear diffusion process into linear latent diffusion by normalizing flows.

Differential Equation Solver Sampler Compared to traditional diffusion methods with discrete steps, numerical formulations of differential equations achieve more efficient sampling with advanced solvers. Inspired by Score SDE and Probability Flow (Diffusion) ODE [53], several works centering on efficient sampling with an advanced differential equation solver by minimizing approximation error using fewer sampling steps. [126], [127], [128], [129] Existing methods can be divided into the ODE-based and the SDE-base. The SDE-based utilize formulation in score SDE along with solvers like Euler-Maruyama (EM) [130], improved Euler, and stochastic Runge-Kutta (RK) [131]method. The ODE-based have a wider range of choices such as Runge-Kutta [132], Forward Euler, and Linear multi-step methods [133]. In general, there exists a trade-off between sampling speed and sampling quality [34]. While higher order differential equation solvers have smaller approximation errors and higher order of convergence, linear solvers require less evaluation. [134] Moreover, ODEs are easier and simpler to solver compared to SDEs. Thus, the choice of differential equations together with related solvers counts leads to another way of classification – Accuracy-prior and Speed-prior on ODE, SDE, and semi-linear DE fields.

For the methods preferred accuracy leveraging higher order solver, Itô-Taylor Sampling Scheme [96] has been proposed using a high-order SDE solver. What is different is that the sampler applied ideal derivative substitution to parameterize the score function in a tricky way that avoids higher-order derivative computing.

There are also methods to improve the whole process by applying both linear solvers and higher-order solvers such as Gotta Go Fast [89] and PNDM [64]. It derived an algorithm based to achieve directional guidance on step size adjustment. In the sampling process, the method combined a linear solver (Euler-Maruyama Method) with a higher-order one (Improved Euler Method) with an extrapolation technique to accelerate with less extra computing. It can reach an FID score of less than 3.00 on CIFAR-10 with 150 steps. PNDM has explored that different numerical solvers can share the same gradient. So it explored the linear multi-step method after using 3 steps of a higher-order solver (Runge-Kutta method) in Diffusion ODE. Besides, DPM-solver [50] also leveraged solvers of different orders. Empirically, DPM Solver-Fast (progress with a mixture of different order solvers) performed the best among all the choices. Therefore, a united solver cross alternative orders may have a better performance after well-design.

Furthermore, from the perspective of differential equation choosing, DPM-solver and DEIS [89] created a new viewpoint except for SDE and Diffusion ODE. They claimed that the diffusion ODE can be seen as a semi-linear form by which the discretization errors are reduced. DPM-solver accomplished the SOTA within 50 steps on CIFAR-10 and it can generate a high-quality image (≤ 7 FID score) with 10 steps, which is an extensive upgrade. On the other hand, DEIS improved numerical DDIM with a multi-step PC-sampling method [135] by the usage of exponential integrator [136]. Furthermore, DEIS-tAB3 achieves the SOTA

on CIFAR10 in 5, 10, 15, and 20 steps with the corresponding FID score of 15.37, 4.17, 3.37, and 2.86. Thus, solving the numerical diffusion model by treating it as a semi-linear structure attains the most effective sampling quality.

Dynamic Programming Adjustment Dynamic programming achieves the traversal of all choices to find the optimized solution in a very reduced time by memorization trick [137]. Compared to other efficient sampling, methods with dynamic programming locate the optimized sampling route instead of designing powerful steps that minimize the error more quickly. Assume that each path from one state to another shares the same KL-Divergence with others, Watson *et al.*, [59] proposed an efficient sampling method to directly search the optimized route of sampling with the minimum ELBO. This method only requires $O(T^2)$ for computing and restoration, and it explores a new approach for optimizing the trajectory. However, the minimization on ELBO sometimes has a mismatch with FID scores [138]. Inspired by Kumar *et al.*, [139] differentiable Diffusion Sampler Search (DDSS) [97] utilizes rematerialization trick to trade memory cost for computation time.

3.1.3 Mixed-Modeling

Mixed-Modeling means pulling another type of generative model in the pipeline of the diffusion model to take virtue of the high sampling speed of others such as adversarial training network and auto-regressive encoder and high expressiveness like normalizing flow. Thus, extracting all the strengths by jointly combining two or more models with a specific pattern performs a promising enhancement, which is called Mixed-modeling. Mixed modeling can be classified into two classes from the perspective of mixing purpose: acceleration mixture and expressiveness mixture.

Acceleration Mixture Acceleration mixture aims at applying high-speed generation of VAEs and GANs to save plenty of steps on the reconstruction of less perturbed data distribution. Existing GAN-based methods consist of two parts as before: the generator is responsible for generating samples x'_0 to be diffused into x'_{t-1} which is as close as x_{t-1} , while the discriminator aims at distinguishing x'_{t-1} and x_{t-1} under the condition of x_t along with $q(x_t|x_{t-1})$. Denoised diffusion GAN [49] became the first DDPM-related model that generated samples with 4 steps, and it obtained an FID score of 9.63 on the CIFAR-10 Dataset. Following a similar pattern, VAE-based models like DiffuseVAE [98] and ES-DDPM [51] apply. Since it takes much time on predicting x_0 in each sampling step when we use $q(x_{t-1}|x_t, x_0)$, VAEs are used in x_0 generation so as to accelerate the whole process, which is what DiffuseVAE has done. Based on DiffuseVAE, ES-DDPM combined the early stop idea in sample trajectory learning and DiffuseVAE to accomplish early stop sampling with the condition generated from diffused VAE samples.

Expressiveness Mixture Another category of mixed-modeling called expressiveness mixture support diffusion models on expressing data or noise in a different pattern. As for noise modulation, DiffFlow [99] employs a flow function in each SDE-based diffusion step forward and backward to add noise adaptively and efficiently by minimizing the KL-

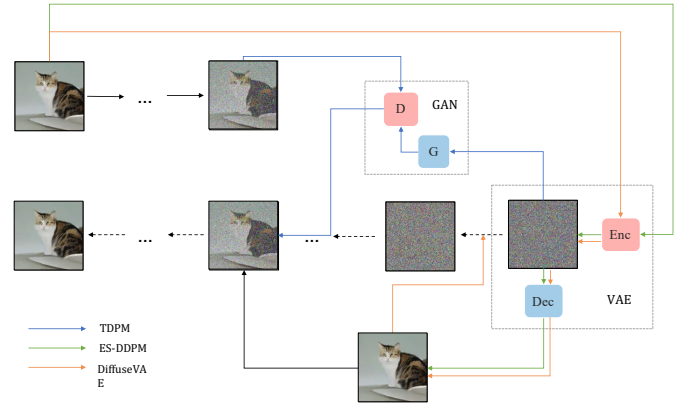


Fig. 4. Acceleration mixed-modeling pipeline. To some extent, this type of model has incomplete diffusion and reverse processes. The blue line represents the pipeline of TDPM. The partly perturbed data x_t is applied as the ground-truth condition for GAN’s generator, and the conditional samples x'_t with the same level of perturbation are generated from the latent before being compared with x_t . The successful samples are applied as the beginning of the reverse process. Instead of using GAN as the high-speed generator, ES-DDPM follows the pattern of TDPM’s with VAE, which is shown with green lines. Besides, DiffuseVAE employs VAE to generate condition x_0 in each sampling step.

Divergence between the forward process and backward process. DiffFlow leads to a 20* speedup compared to DDPM, although there is a longer time required per step since the flow functions’ back-propagation. An additional set of models leverage NFs into data transformation. Training data based on its latent space (noncontinuous data) allows us to learn smoother models in a smaller space, triggering fewer network evaluations and faster sampling [100]. Therefore, both LSGM [100] and PDM [102] obtained latent variables using VAE and flow function respectively. Besides, based on the goal of Maximal Likelihood Estimation (MLE), LSGM jointly trained the diffusion process along with VAE, while PDM jointly trained the SDE of score matching along with the invertible normalizing flow. Besides, Score-Flow [101] employs normalizing flow to transform data distribution into a dequantization field and conduct a diffusion process to generate dequantized samples. Projecting data onto the dequantization field with variational dequantization solves the mismatching between continuous density and discrete data [140], [141], eliminating the gap between dequantization space and discrete space, leading to enhancement of sample quality [142], [143].

3.1.4 Score & Diffusion Unification

There are many works on unifying the diffusion models with a generalized one. The acceleration method on generalized diffusion helps a lot in solving a wide range of models along with insights into efficient sampling mechanisms. Also, other related works determine the connection between the diffusion model and denoising score matching, which can be viewed as one type of unification.

For generalized perspective, FastDPM [89] and VDM [54] finished the unification w.r.t. noise schedules. In FastDPM, there is a bijective mapping between continuous-time and noise scale. So, the diffusion and reverse parameterization is accomplished by noise scale defined by $r : r = \mathcal{R}(t)$ and $t = \mathcal{T}(r)$. VDM first proposed the signal-

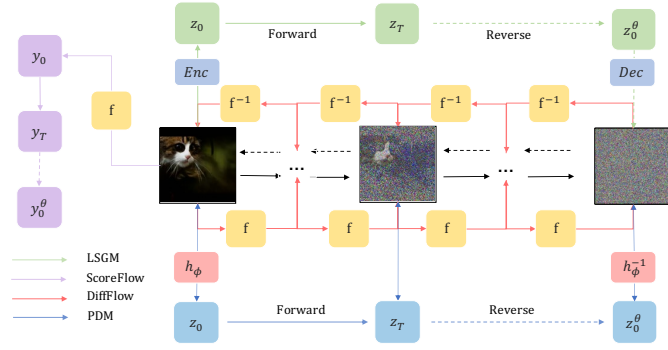


Fig. 5. Expressiveness mixed-modeling pipeline. The models for expressiveness enhancement keep the same procedure as DDPM in the training, diffusion, and sampling process, which is denoted by black lines. Furthermore, additional improvements are highlighted by other colors. The red lines show the pipeline of DiffFlow, which adds flow function and related inverse function at each step. The works in blue lines and green lines represent the idea of latent space diffusion by jointly training mixture models. Different supporting generative models are used in LSGM and PDM. Besides, Score-Flow uses the flow function as a projector from discrete space to dequantization space. Then generating dequantized samples using the traditional diffusion method.

TABLE 3
Benchmarks on CelebA-64

Method	NFE	FID	NLL
NCSN [55]	1000	10.23	-
NCSN ++ [144]	1000	1.92	1.97
DDPM ++ [144]	1000	1.90	2.10
DiffuseVAE [98]	1000	4.76	-
Analytic DPM [92]	1000	-	2.66
ES-DDPM [51]	200	2.55	-
PNDM [64]	200	2.71	-
ES-DDPM [51]	100	3.01	-
PNDM [64]	100	2.81	-
Analytic DPM [92]	100	-	2.66
ES-DDPM [51]	50	3.97	-
PNDM [64]	50	3.34	-
DPM-Solver Discrete [50]	36	2.71	-
ES-DDPM [51]	20	4.90	-
PNDM [64]	20	5.51	-
DPM-Solver Discrete [50]	20	2.82	-
ES-DDPM [51]	10	6.44	-
PNDM [64]	10	7.71	-
Analytic DPM [92]	10	-	2.97
DPM-Solver Discrete [50]	10	6.92	-
ES-DDPM [51]	5	9.15	-
PNDM [64]	5	11.30	-

to-noise ratio (SNR) parameterization criteria, revealing the effects of the noise scheme on the diffusion model’s training and sampling. Generalized DDIM (gDDIM) [94] unifies the DDIM family with according to the transition kernel during each step.

From the unification perspective, score SDE [53] is the landmark work that combines two types of problems into one along with proposing a unified framework. Gong *et al.*, [104] reveals the hidden connection between score matching with the normalizing flow, and it provides a new approach to expressing score matching by flow ODEs [63], [124]. Bortoli *et al.*, [103] provided a variational score matching approach for simulating diffusion bridges using Doob-h transformation [189].

TABLE 4
Benchmarks on ImageNet-64

Method	NFE	FID	IS	NLL
MCG [145]	1000	25.4	-	-
Analytic DPM [92]	1000	-	-	3.61
ES-DDPM [51]	900	2.07	55.29	-
Efficient Sampling [59]	256	3.87	-	-
Analytic DPM [92]	200	-	-	3.64
ES-DDPM [51]	100	3.75	48.63	-
DPM-Solver Discrete [50]	57	17.47	-	-
ES-DDPM [51]	25	3.75	48.63	-
GGDM [97]	25	18.4	18.12	-
Analytic DPM [92]	25	-	-	3.83
DPM-Solver Discrete [50]	20	18.53	-	-
ES-DDPM [51]	10	3.93	48.81	-
GGDM [97]	10	37.32	14.76	-
DPM-Solver Discrete [50]	10	24.4	-	-
ES-DDPM [51]	5	4.25	48.04	-
GGDM [97]	5	55.14	12.9	-

3.2 Distribution Diversification

Currently, most improvement methods for acceleration and computation cost reduction concentrate on the performance of RGB-image data in order to evaluate the power of generation. Indeed, most kinds of existing data can be the input of diffusion models, leading to various applications in the other fields, such as amino acid residue [186], audio sequence [177], and torsion angle [184]. More importantly, the traditional patterns of diffusion which utilize Gaussian distribution as prior and transition kernel are to be extended to explore the influences of patterns with distinct distributions. However, works on this topic are relatively less. Thus, we divided the distribution diversification into three aspects: discrete space, continuous space, and Constrained space with structural constraints.

3.2.1 Continuous Space

For continuous space methods, two main classes – Dequantization space and point cloud space are introduced. As mentioned above, dequantization space projection solves the mismatching between continuous density and discrete data [140], [141] as well as eliminates the gap between dequantization space and discrete space, leading to enhancement of sample quality [142], [143]. Point cloud data used for 3d shape generation, 3d shape completion, and multi-modal completion attract more attention but meet the barrier using the autoregressive encoder and normalizing flows due to the irregular sampling procedure. Diffusion models applied to continuous space data often combine other projection networks such as VAE and normalizing flow to transform various types of data into specific latent spaces.

Dequantization & Point Cloud Score-flow [101] employs flow function to project RGB-image into dequantization space, achieving diffusion techniques on it for generating accurate samples. Point cloud generation is firstly proposed by Luo *et al.* [106], which generates latent samples for point cloud data, and conducts transformation to obtain high-quality 3d shapes. Other techniques such as [105], [107], [108] accomplish the shape generation and completion tasks in similar ways. Some slight improvements used in latent space transformation such as canonical map [108], condition

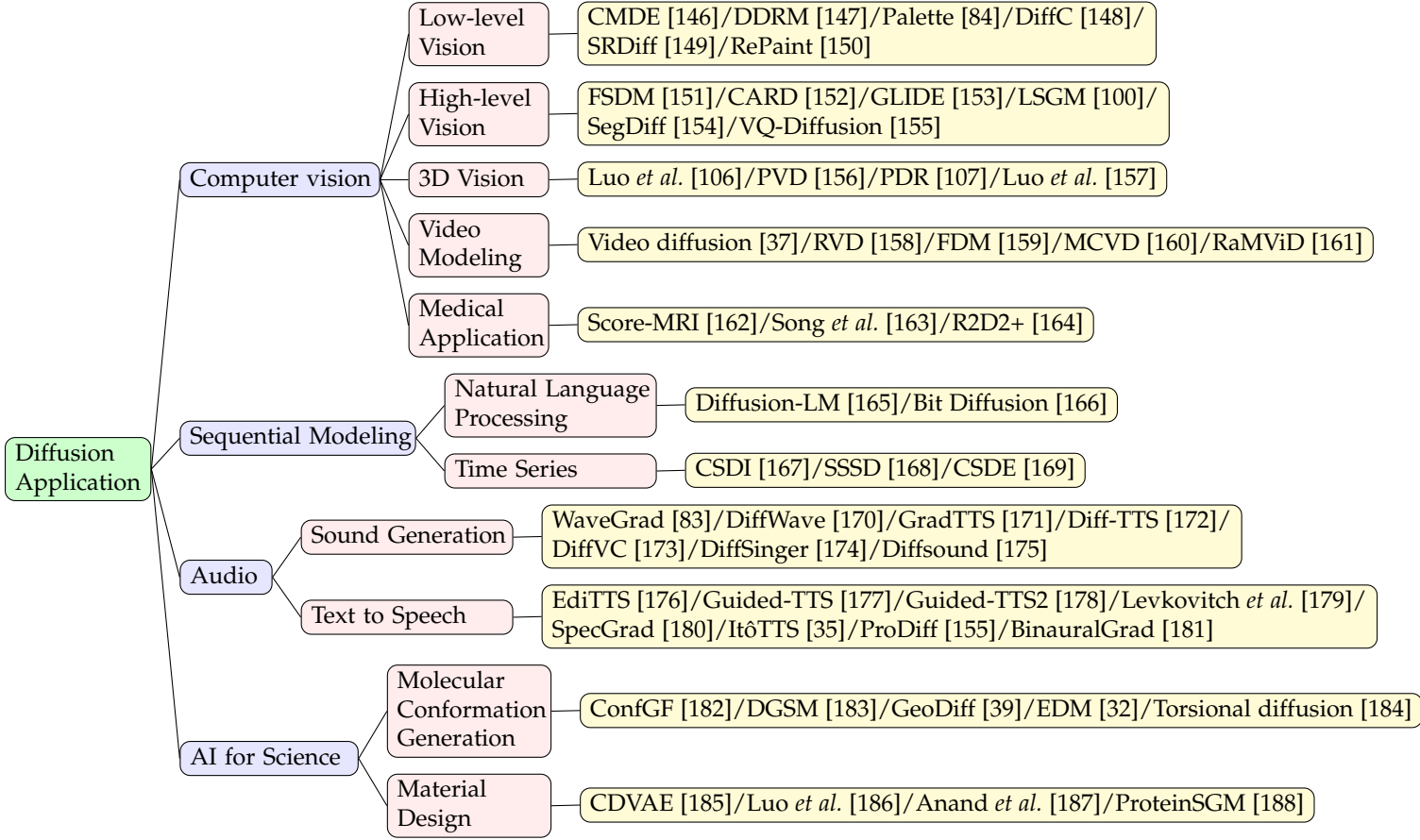


Fig. 6. Classification of Diffusion-based model Applications

feature extraction sub-nets [107], and point-voxel representation [105].

Latent Space Similar to Expressiveness mixture modeling, latent space data distributions are often processed for diffusion application since different types of complex data structures require a unified approach to generalize and analyze. Most current methods project data into continuous space, and they obtain promising performance with the aid of high-quality generation power of diffusion models such as EDM [32] and antigen-diffusion [33]. Thus, latent space processing should be a beneficial pattern utilized in new application fields.

3.2.2 Discrete Space

Text & Categorical For discrete space methods, they focus on combining different types of data structures such as vector-quantized data, text data, and categorical data into the diffusion model’s training and sampling so as to handle a wider range of field tasks such as text, segmentation maps, and categorical features [111].D3PM [91] firstly promoted diffusion algorithm onto discrete space to deal with discrete data like sentences and images by means of defining

$$q(x_t | x_{t-1}) = \text{Cat}(x_t; p = x_{t-1} \mathbf{Q}_t) \quad (43)$$

where $[\mathbf{Q}_t]_{ij} = q(x_t = j | x_{t-1} = i)$ is defined as the transition, and $\text{Cat}(\cdot)$ is defined as the categorical distribution

over the one-hot row vector.

Besides, in order to process multi-nominal discrete data as well as promote better predictions of the data x_0 at each time step, the parameterization and training objectives are:

$$p_\theta(x_{t-1} | x_t) \propto \sum_{\tilde{x}_0} q(x_{t-1}, x_t | \tilde{x}_0) \tilde{p}_\theta(\tilde{x}_0 | x_t) \quad (44)$$

$$L_\lambda = L_{\text{vb}} + \lambda \mathbb{E}_{q(x_0)} \mathbb{E}_{q(x_t | x_0)} [-\log \tilde{p}_\theta(x_0 | x_t)] \quad (45)$$

Similar to D3PM, multi-nomial diffusion [109] and ARDM [110] extended the categorical diffusion into multinomial data for generating language text & segmentation map and Lossless Compression.

Vector-Quantized To handle the multi-model problem, vector-quantized (VQ) data is proposed to combine data from different fields into the codebook. VQ data processing achieved great performance in autoregressive encoders [190]. Gu *et al.* [112] firstly applied diffusion techniques into VQ data, solving unidirectional bias as well as accumulation prediction error problems existing in VQ-VAE. Further works such as Xie *et al.* [115], Cohen *et al.* [114], and Improved VQ-Diffusion [113] accomplished text-to-sign pose generation, diffusion-bridge generation through VQ-VAE pipeline, and inference strategy improvement respectively by re-defining the transition process as:

$$q(x_t | x_{t-1}) = \mathbf{v}^\top(x_t) \mathbf{Q}_t \mathbf{v}(x_{t-1}) \quad (46)$$

where $v(t)$ is a one-hot vector of the equal length with the code-book, and $Q(t)$ is called the probability transition matrix:

$$Q_t = \begin{bmatrix} \alpha_t + \beta_t & \beta_t & \beta_t & \cdots & 0 \\ \beta_t & \alpha_t + \beta_t & \beta_t & \cdots & 0 \\ \beta_t & \beta_t & \alpha_t + \beta_t & \cdots & 0 \\ \vdots & \vdots & \vdots & \ddots & \vdots \\ \gamma_t & \gamma_t & \gamma_t & \cdots & 1 \end{bmatrix} \quad (47)$$

Training methods are similar to DDPM’s but with a new expression scheme.

3.2.3 Constrained Space

Riemann Space Most currently data structures such as image and text are defined in Euclidean space, which is a flat-geometry manifold. However, there exists a series of data in the field of robotics [191], [192], geoscience [193], [194], [195], and protein modelling [196] defined in Riemannian manifold [197], where existing methods for Euclidean space cannot capture the feature of sphere well. Thus, recent methods RDM [117] and RGSM [116] applied diffusion techniques into Riemannian manifold by score SDE framework [53] with a slight change. The revised SDE system is defined by:

$$d\mathbf{X}_t = b(\mathbf{X}_t) dt + d\mathbf{B}_t^M \quad (48)$$

The time-reverse process is defined as:

$$d\mathbf{Y}_t = \{-b(\mathbf{Y}_t) + \nabla \log p_{T-t}(\mathbf{Y}_t)\} dt + d\mathbf{B}_t^M \quad (49)$$

The corresponding sampling algorithm called Geodesic Random Walk (GRW) [198], [199], [200] is implemented:

$$X_{n+1}^\gamma = \exp_{X_n^\gamma} \left[\gamma \{b(X_n^\gamma) + (1/\sqrt{\gamma})(V_{n+1} - b(X_n^\gamma))\} \right] \quad (50)$$

Unlike the above two methods, PNDM [64] draws support from Manifold space to solve neural differential equation for sampling, which indeed is a generalized version for differential equation sampler [201].

Graph According to [202], graph is becoming an increasingly popular topic but few works are proposed in the field of diffusion. In EDP-GNN [118], graph data is processed through an adjacency matrix before being applied in the traditional discrete score matching pipeline in order to capture the graph’s permutation invariance.

3.3 Benchmarks

The benchmarks of landmark models along with improved techniques corresponding to FID score, Inception Score, and NLL are provided on diverse datasets which includes CIFAR-10 [203], ImageNet [204], and CelebA-64 [205]. In addition, some dataset-based performances such as LSUN [206], FFHQ [207], and MINST [208] are not presented since there is much less experiment data. The selected performance are listed according to NFE in descending order in order to compare for easier access.

4 APPLICATION

Benefiting from the powerful ability to generate realistic samples, diffusion models have been widely used in various fields such as computer vision, natural language processing, and bioinformatics.

4.1 Computer vision

4.1.1 Low-level vision

CMDE [146] empirically compared score-based diffusion methods in modeling conditional distributions of visual image data and introduced a multi-speed diffusion framework. By leveraging the controllable diffusion speed of the condition, CMDE outperformed the vanilla conditional denoising estimator [55] in terms of FID scores in in-painting and super-resolution tasks. DDRM [147] proposed an efficient, unsupervised posterior sampling method served for image restoration. Motivated by variational inference, DDRM demonstrated successful applications in super-resolution, deblurring, inpainting, and colorization of diffusion models. Palette [84] further developed a unified diffusion-based framework for low-level vision tasks such as colorization, inpainting, cropping, and restoration. With its simple and general idea, this work demonstrated the superior performance of diffusion models compared to GAN models. DiffC [148] proposed an unconditional generative approach that encoded and denoise corrupted pixels with a single diffusion model, which showed the potential of diffusion models in lossy image compression. SRDiff [149] exploited the diffusion-based single-image super-resolution model and showed competitive results. RePaint [150] was a free-form inpainting method that directly employed a pre-trained diffusion model as the generative prior and only replaced the reverse diffusion by sampling the unmasked regions using the given image information. Though there was no modification to the vanilla pre-trained diffusion model, this method was able to outperform autoregressive and GAN methods under extreme tasks.

4.1.2 High-level vision

FSDM [151] was a few-shot generation framework based on conditional diffusion models. Leveraging advances in vision transformers and diffusion models, FSDM can adapt quickly to various generative processes at test-time and performs well under few-shot generation with strong transfer capability. CARD [152] proposed classification and regression diffusion models, combining a denoising diffusion-based conditional generative model and a pre-trained conditional mean estimator to predict data distribution under given conditions. Though approaching supervised learning from a conditional generation perspective and training with objectives indirectly related to the evaluation metrics, CARD presented a strong ability in uncertainty estimation with the help of diffusion models. Motivated by CLIP [209], GLIDE [153] explored realistic image synthesis conditioned on the text and found that diffusion models with classifier-free guidance yielded high-quality images containing a wide range of learned knowledge. To obtain expressive generative models within a smooth and limited space, LSGM [100] built a diffusion model trained in the latent space with the help of a variational autoencoder framework.

SegDiff [154] extended diffusion models for performing image-level segmentation by summing up feature maps from a diffusion-based probabilistic encoder and an image feature encoder. Video diffusion [37], on the other hand, extended diffusion models in the time axis and performed video-level generation by utilizing a typically designed reconstruction-guided conditional sampling method. VQ-Diffusion [155] improved vanilla vector quantized diffusion by exploring classifier-free guidance sampling for discrete diffusion models and presenting a high-quality inference strategy. This method showed superior performance on large datasets such as ImageNet [204] and MSCOCO [210].

4.1.3 3D vision

[106] was an early work on diffusion-based 3D vision tasks. Motivated by the non-equilibrium thermodynamics, this work analogized points in point clouds as particles in a thermodynamic system and employed the diffusion process in point cloud generation, which achieved competitive performance. PVD [156] was a concurrent work on diffusion-based point cloud generation but performed unconditional generation without additional shape encoders, while a hybrid and point-voxel representation was employed for processing shapes. PDR [107] proposed a paradigm for diffusion-based point cloud completion that applied a diffusion model to generate a coarse completion based on the partial observation and refined the generated output by another network. To deal with point cloud denoising, [157] introduced a neural network to estimate the score of the distribution and denoised point clouds by gradient ascent.

4.1.4 Video modeling

Video diffusion [37] introduced the advances in diffusion-based generative models into the video domain. RVD [158] employed diffusion models to generate a residual to a deterministic next-frame prediction conditioned on the context vector. FDM [159] applied diffusion models to assist long video prediction and performed photo-realistic videos. MCVD [160] proposed a conditional video diffusion framework for video prediction and interpolation based on masking frames in a blockwise manner. RaMViD [161] extended image diffusion models to videos with 3D convolutional neural networks and designed a conditioning technique for video prediction, infilling, and upsampling.

4.1.5 Medical application

It is a natural choice to apply diffusion models to medical images. Score-MRI [162] proposed a diffusion-based framework to solve magnetic resonance imaging (MRI) reconstruction. [163] was a concurrent work but provided a more flexible framework that did not require a paired dataset for training. With a diffusion model trained on medical images, this work leveraged the physical measurement process and focused on sampling algorithms to create image samples that are consistent with the observed measurements and the estimated data prior. R2D2+ [164] combined diffusion-based MRI reconstruction and super-resolution into the same network for end-to-end high-quality medical image generation.

4.2 Sequential modeling

4.2.1 Natural language processing

Benefited by the non-autoregressive mechanism of diffusion models, Diffusion-LM [165] took advantage of continuous diffusions to iteratively denoise noisy vectors into word vectors and performed controllable text generation tasks. Bit Diffusion [166] proposed a diffusion model for generating discrete data and was applied to image caption tasks.

4.2.2 Time series

To deal with time series imputation, CSDI [167] utilized score-based diffusion models conditioned on observed data. Inspired by masked language modeling, a self-supervised training procedure was developed that separates observed values into conditional information and imputation targets. SSSD [168] further introduced structured state space models to capture long-term dependencies in time series data. CSDE [169] proposed a probabilistic framework to model stochastic dynamics and introduced Markov dynamic programming and multi-conditional forward-backward losses to generate complex time series.

4.3 Audio

WaveGrad [83] and DiffWave [170] were seminal works that applied diffusion models to raw waveform generation and obtained superior performance. GradTTS [171] and DiffTTS [172] also implemented diffusion models but generated mel feature instead of raw waves. DiffVC [173] further challenged the one-shot many-to-many voice conversion problem and developed a stochastic differential equation solver. DiffSinger [174] extended the common sound generation to singing voice synthesis based on a shallow diffusion mechanism. Diffsound [175] proposed a sound generation framework conditioned on the text that employed a discrete diffusion model to replace the autoregressive decoder to overcome the unidirectional bias and accumulated errors. EdiTTS [176] was also a diffusion-based audio model for the text-to-speech task. Through coarse perturbations in the prior space, desired edits were induced during denoising reversal. Guided-TTS [177] and Guided-TTS2 [178] were also an early series of text-to-speech models that successfully applied diffusion models in sound generation. [179] combined a voice diffusion model with a spectrogram-domain conditioning method and performed text-to-speech with voices unseen during training. InferGrad [211] considered the inference process in training and improved the diffusion-based text-to-speech model when the number of inference steps is small, enabling fast and high-quality sampling. SpecGrad [180] brought ideas from signal processing and adapted the time-varying spectral envelope of diffusion noise based on the conditioning log-mel spectrogram. ItôTTS [35] unified text-to-speech and vocoder into a framework based on linear SDE. ProDiff [155] proposed a progressive and fast diffusion model for high-quality text-to-speech. Instead of hundreds of iterations, ProDiff parameterized the model by predicting clean data and employed a teacher-synthesized mel-spectrogram as a target to reduce data discrepancies and make a sharp prediction. Binaural-Grad [181] was a two-stage diffusion-based framework that

explored the application of diffusion models in binaural audio synthesis given mono audio.

4.4 AI for science

4.4.1 Molecular conformation generation

ConfGF [182] was an early work on diffusion-based molecular conformation generation models. While preserving rotation and translation equivariance, ConfGF generated samples by Langevin dynamics with physically inspired gradient fields. However, ConfGF only modeled local distances between the first-order, the second-order, and the third-order neighbors and thus failed to capture long-range interactions between non-bounded atoms. To tackle this challenge, DGSM [183] proposed to dynamically construct molecular graph structures between atoms based on their spatial proximity. GeoDiff [39] found that the model was fed with perturbed distance matrices during diffusion learning, which might violate mathematical constraints. Thus, GeoDiff introduced a roto-translational invariant Markov process to impose constraints on the density. EDM [32] further extended the above methods by incorporating discrete atom features and deriving the equations required for log-likelihood computation. Torsional diffusion [184] operated on the space of torsional angles and produced molecular conformations according to a diffusion process limited to the most flexible degrees of freedom.

4.4.2 Material design

CDVAE [185] explored the periodic structure of stable material generation. To address the challenge that stable materials exist only in a low-dimensional subspace with all possible periodic arrangements of atoms, CDVAE designed a diffusion-based network as a decoder with output gradients leading to local minima of energy and updated atom types to capture specific local bonding preferences depending on the neighbors.

Inspired by the recent success of antibody modeling [212], [213], [214], the recent work [186] developed a diffusion-based generative model that explicitly targeted specific antigen structures and generated antibodies. The proposed method jointly sampled antibody sequences and structures and iteratively generated candidates in the sequence-structure space.

Anand *et al.* [187] introduced a diffusion-based generative model for both protein structure and sequence and learned the structural information that is equivariant to rotations and translations. ProteinSGM [188] formulated protein design as an image inpainting problem and applied conditional diffusion-based generation to precisely model the protein structure.

5 CONCLUSIONS & DISCUSSIONS

The diffusion model is becoming a popular topic in a wide range of application fields. To utilize the power of the diffusion model, this paper provides a comprehensive and up-to-date review of several aspects of diffusion models using detailed insights on various attitudes, including theory, improved algorithms, and applications. We hope this survey serves as a guide for readers on diffusion model enhancement and model enhancement.

5.1 Limitations

There is already a wide range of improved techniques and application fields based on diffusion models. However, more attention to fast sampling leads to less effectiveness in training schemes and original settings. Firstly, there's a variational gap defined by the difference between negative log-likelihood and evidence lower bound. Most current works focus on optimizing ELBO but ignore the minimization task on variation gap, while there is still a relatively huge space to be optimized. Secondly, there's a mismatch between the training objective and evaluation metric performance. Sometimes, the lower loss does not bring higher quality. Thus, mechanisms for unifying the two terms are to be explored, including connection indication and metric improvement. Thirdly, existing works have not paid much attention to noise types and perturbation kernels' types. Instead, Gaussian perturbation, as well as the final state as Gaussian noise, are the most likely to be used, where we have no idea if Gaussian noise is reasonable in some specific tasks. More attention should be drawn to it. Finally, the trade-off between model speed and sampling quality is still unclear and unquantified. The optimization task on quantitative trade-offs may provide insight into adjusting the models' efficiency.

5.2 Further Directions

From the perspective of algorithm and application, we present some expected directions in this subsection. On the one hand, there should be more tries on different data types including discrete space, dequantization space, and latent space. Also, experiments for exploring diverse final state noise types and perturbation kernels are needed such as normal distribution, Bernoulli distribution, binomial distribution, and Poisson distribution to broaden diffusion model diversity. Besides, a clear mechanism for loss optimization along with acceleration & quality trade-off will lead to promising influences on controllable regulation and more satisfying performance. On the other hand, there are various fields where diffusion models have been employed in order to obtain better generation performance. However, most of the current applications remain superficial. More problem-specific diffusion models are expected, especially for scientific problems.

ACKNOWLEDGMENTS

This work is supported by the Science and Technology Innovation 2030 - Major Project (No. 2021ZD0150100) and the National Natural Science Foundation of China (No. U21A20427).

We appreciate Dr. Jindong Wang provided the idea for our classification figures.

REFERENCES

- [1] D. J. Rezende, S. Mohamed, and D. Wierstra, "Stochastic back-propagation and approximate inference in deep generative models," in *International conference on machine learning*. PMLR, 2014, pp. 1278–1286. (document)
- [2] C. Doersch, "Tutorial on variational autoencoders," *arXiv preprint arXiv:1606.05908*, 2016. (document)

- [3] D. P. Kingma, M. Welling *et al.*, “An introduction to variational autoencoders,” *Foundations and Trends® in Machine Learning*, vol. 12, no. 4, pp. 307–392, 2019. (document)
- [4] A. Oussidi and A. Elhassouny, “Deep generative models: Survey,” in *2018 International Conference on Intelligent Systems and Computer Vision (ISCV)*. IEEE, 2018, pp. 1–8. (document)
- [5] Y. LeCun, S. Chopra, R. Hadsell, M. Ranzato, and F. Huang, “A tutorial on energy-based learning,” *Predicting structured data*, vol. 1, no. 0, 2006. (document)
- [6] J. Ngiam, Z. Chen, P. W. Koh, and A. Y. Ng, “Learning deep energy models,” in *Proceedings of the 28th international conference on machine learning (ICML-11)*, 2011, pp. 1105–1112. (document)
- [7] A. G. ALIAS PARTH GOYAL, N. R. Ke, S. Ganguli, and Y. Bengio, “Variational walkback: Learning a transition operator as a stochastic recurrent net,” *Advances in Neural Information Processing Systems*, vol. 30, 2017. (document)
- [8] T. Kim and Y. Bengio, “Deep directed generative models with energy-based probability estimation,” *arXiv preprint arXiv:1606.03439*, 2016. (document)
- [9] J. Zhao, M. Mathieu, and Y. LeCun, “Energy-based generative adversarial network,” *arXiv preprint arXiv:1609.03126*, 2016. (document)
- [10] J. Xie, Y. Lu, S.-C. Zhu, and Y. Wu, “A theory of generative convnet,” in *International Conference on Machine Learning*. PMLR, 2016, pp. 2635–2644. (document)
- [11] R. Gao, Y. Lu, J. Zhou, S.-C. Zhu, and Y. N. Wu, “Learning generative convnets via multi-grid modeling and sampling,” in *Proceedings of the IEEE Conference on Computer Vision and Pattern Recognition*, 2018, pp. 9155–9164. (document)
- [12] R. Kumar, S. Ozair, A. Goyal, A. Courville, and Y. Bengio, “Maximum entropy generators for energy-based models,” *arXiv preprint arXiv:1901.08508*, 2019. (document)
- [13] E. Nijkamp, M. Hill, S.-C. Zhu, and Y. N. Wu, “Learning non-convergent non-persistent short-run mcmc toward energy-based model,” *Advances in Neural Information Processing Systems*, vol. 32, 2019. (document)
- [14] Y. Du and I. Mordatch, “Implicit generation and generalization in energy-based models,” *arXiv preprint arXiv:1903.08689*, 2019. (document)
- [15] W. Grathwohl, K.-C. Wang, J.-H. Jacobsen, D. Duvenaud, M. Norouzi, and K. Swersky, “Your classifier is secretly an energy based model and you should treat it like one,” *arXiv preprint arXiv:1912.03263*, 2019. (document)
- [16] G. Desjardins, Y. Bengio, and A. C. Courville, “On tracking the partition function,” *Advances in neural information processing systems*, vol. 24, 2011. (document)
- [17] R. Gao, E. Nijkamp, D. P. Kingma, Z. Xu, A. M. Dai, and Y. N. Wu, “Flow contrastive estimation of energy-based models,” in *Proceedings of the IEEE/CVF Conference on Computer Vision and Pattern Recognition*, 2020, pp. 7518–7528. (document)
- [18] T. Che, R. Zhang, J. Sohl-Dickstein, H. Larochelle, L. Paull, Y. Cao, and Y. Bengio, “Your gan is secretly an energy-based model and you should use discriminator driven latent sampling,” *Advances in Neural Information Processing Systems*, vol. 33, pp. 12 275–12 287, 2020. (document)
- [19] Y. Qiu, L. Zhang, and X. Wang, “Unbiased contrastive divergence algorithm for training energy-based latent variable models,” in *International Conference on Learning Representations*, 2019. (document)
- [20] B. Rhodes, K. Xu, and M. U. Gutmann, “Telescoping density-ratio estimation,” *Advances in neural information processing systems*, vol. 33, pp. 4905–4916, 2020. (document)
- [21] L. Jin, J. Lazarow, and Z. Tu, “Introspective classification with convolutional nets,” *Advances in Neural Information Processing Systems*, vol. 30, 2017. (document)
- [22] I. Goodfellow, J. Pouget-Abadie, M. Mirza, B. Xu, D. Warde-Farley, S. Ozair, A. Courville, and Y. Bengio, “Generative adversarial networks,” *Communications of the ACM*, vol. 63, no. 11, pp. 139–144, 2020. (document)
- [23] A. Creswell, T. White, V. Dumoulin, K. Arulkumaran, B. Sengupta, and A. A. Bharath, “Generative adversarial networks: An overview,” *IEEE signal processing magazine*, vol. 35, no. 1, pp. 53–65, 2018. (document)
- [24] J. Gui, Z. Sun, Y. Wen, D. Tao, and J. Ye, “A review on generative adversarial networks: Algorithms, theory, and applications,” *IEEE Transactions on Knowledge and Data Engineering*, 2021. (document)
- [25] L. Dinh, J. Sohl-Dickstein, and S. Bengio, “Density estimation using real nvp,” *arXiv preprint arXiv:1605.08803*, 2016. (document)
- [26] D. Rezende and S. Mohamed, “Variational inference with normalizing flows,” in *International conference on machine learning*. PMLR, 2015, pp. 1530–1538. (document)
- [27] I. Kobyzev, S. J. Prince, and M. A. Brubaker, “Normalizing flows: An introduction and review of current methods,” *IEEE transactions on pattern analysis and machine intelligence*, vol. 43, no. 11, pp. 3964–3979, 2020. (document)
- [28] S. Bond-Taylor, A. Leach, Y. Long, and C. Willcocks, “Deep generative modelling: A comparative review of vaes, gans, normalizing flows, energy-based and autoregressive models,” *IEEE Transactions on Pattern Analysis and Machine Intelligence*, 2021. (document)
- [29] G. Papamakarios, E. T. Nalisnick, D. J. Rezende, S. Mohamed, and B. Lakshminarayanan, “Normalizing flows for probabilistic modeling and inference,” *J. Mach. Learn. Res.*, vol. 22, no. 57, pp. 1–64, 2021. (document), 1
- [30] C. Winkler, D. Worrall, E. Hoogeboom, and M. Welling, “Learning likelihoods with conditional normalizing flows,” *arXiv preprint arXiv:1912.00042*, 2019. (document)
- [31] C. Saharia, W. Chan, H. Chang, C. A. Lee, J. Ho, T. Salimans, D. J. Fleet, and M. Norouzi, “Palette: Image-to-image diffusion models,” 2021. [Online]. Available: <https://arxiv.org/abs/2111.05826> (document)
- [32] E. Hoogeboom, V. G. Satorras, C. Vignac, and M. Welling, “Equivariant diffusion for molecule generation in 3d,” in *International Conference on Machine Learning*. PMLR, 2022, pp. 8867–8887. (document), 3.1.3, 3.2.1, 4.4.1
- [33] S. Luo, Y. Su, X. Peng, S. Wang, J. Peng, and J. Ma, “Antigen-specific antibody design and optimization with diffusion-based generative models,” *bioRxiv*, 2022. [Online]. Available: <https://www.biorxiv.org/content/early/2022/07/11/2022.07.10.499510> (document), 3.2.1
- [34] H. Tachibana, M. Go, M. Inahara, Y. Katayama, and Y. Watanabe, “It^o-taylor sampling scheme for denoising diffusion probabilistic models using ideal derivatives,” *arXiv preprint arXiv:2112.13339*, 2021. (document), 2, 3.1.2
- [35] S. Wu and Z. Shi, “It^ots and it^owave: Linear stochastic differential equation is all you need for audio generation,” *arXiv e-prints*, pp. arXiv–2105, 2021. (document), 3.1.3, 4.3
- [36] J. Sohl-Dickstein, E. Weiss, N. Maheswaranathan, and S. Ganguli, “Deep unsupervised learning using nonequilibrium thermodynamics,” in *International Conference on Machine Learning*. PMLR, 2015, pp. 2256–2265. (document), 2.1.4
- [37] J. Ho, T. Salimans, A. A. Gritsenko, W. Chan, M. Norouzi, and D. J. Fleet, “Video diffusion models,” in *ICLR Workshop on Deep Generative Models for Highly Structured Data*, 2022. (document), 3.1.3, 4.1.2, 4.1.4
- [38] B. L. Trippe, J. Yim, D. Tischer, D. Baker, T. Broderick, R. Barzilay, and T. Jaakkola, “Diffusion probabilistic modeling of protein backbones in 3d for the motif-scaffolding problem,” 2022. [Online]. Available: <https://arxiv.org/abs/2206.04119> (document)
- [39] M. Xu, L. Yu, Y. Song, C. Shi, S. Ermon, and J. Tang, “Geodiff: A geometric diffusion model for molecular conformation generation,” in *International Conference on Learning Representations*, 2021. (document), 3.1.3, 4.4.1
- [40] Z. Kong, W. Ping, J. Huang, K. Zhao, and B. Catanzaro, “Diffwave: A versatile diffusion model for audio synthesis,” 2020. [Online]. Available: <https://arxiv.org/abs/2009.09761> (document)
- [41] H. Kim, S. Kim, and S. Yoon, “Guided-tts: A diffusion model for text-to-speech via classifier guidance,” 2021. [Online]. Available: <https://arxiv.org/abs/2111.11755> (document)
- [42] P. Dhariwal and A. Nichol, “Diffusion models beat gans on image synthesis,” *Advances in Neural Information Processing Systems*, vol. 34, pp. 8780–8794, 2021. (document)
- [43] N. Chen, Y. Zhang, H. Zen, R. J. Weiss, M. Norouzi, and W. Chan, “Wavegrad: Estimating gradients for waveform generation,” 2020. [Online]. Available: <https://arxiv.org/abs/2009.00713> (document)
- [44] I. J. Goodfellow, J. Pouget-Abadie, M. Mirza, B. Xu, D. Warde-Farley, S. Ozair, A. Courville, and Y. Bengio, “Generative adversarial networks,” 2014. [Online]. Available: <https://arxiv.org/abs/1406.2661> 1

- [45] I. Goodfellow, Y. Bengio, and A. Courville, *Deep Learning*. MIT Press, 2016, <http://www.deeplearningbook.org>. 1
- [46] D. P. Kingma and M. Welling, "Auto-encoding variational bayes," *arXiv preprint arXiv:1312.6114*, 2013. 1
- [47] A. Q. Nichol and P. Dhariwal, "Improved denoising diffusion probabilistic models," in *International Conference on Machine Learning*. PMLR, 2021, pp. 8162–8171. (document), 2.5.3, 3.1.1, 2, 5, 6
- [48] T. Salimans and J. Ho, "Progressive distillation for fast sampling of diffusion models," *arXiv preprint arXiv:2202.00512*, 2022. (document), 3, 3.1.1, 2, 5
- [49] Z. Xiao, K. Kreis, and A. Vahdat, "Tackling the generative learning trilemma with denoising diffusion gans," *arXiv preprint arXiv:2112.07804*, 2021. (document), 2, 3.1.3, 5
- [50] C. Lu, Y. Zhou, F. Bao, J. Chen, C. Li, and J. Zhu, "Dpm-solver: A fast ode solver for diffusion probabilistic model sampling in around 10 steps," 2022. [Online]. Available: <https://arxiv.org/abs/2206.00927> (document), 2.2.3, 2, 3.1.2, 3, 4, 5
- [51] Z. Lyu, X. Xu, C. Yang, D. Lin, and B. Dai, "Accelerating diffusion models via early stop of the diffusion process," *arXiv preprint arXiv:2205.12524*, 2022. (document), 3.1.1, 2, 3.1.3, 3, 4, 5
- [52] J. Ho, A. Jain, and P. Abbeel, "Denosing diffusion probabilistic models," *CoRR*, vol. abs/2006.11239, 2020. [Online]. Available: <https://arxiv.org/abs/2006.11239> 2.2, 2.2.1, 2.2.1, 2.2.1, 6
- [53] Y. Song, J. Sohl-Dickstein, D. P. Kingma, A. Kumar, S. Ermon, and B. Poole, "Score-based generative modeling through stochastic differential equations," *arXiv preprint arXiv:2011.13456*, 2020. 2.2, 2.2.2, 2.2.2, 2.2.3, 2.4.3, 2, 3.1.2, 3.1.4, 3.2.3, 6
- [54] D. Kingma, T. Salimans, B. Poole, and J. Ho, "Variational diffusion models," *Advances in neural information processing systems*, vol. 34, pp. 21696–21707, 2021. 2.2.1, 3.1.1, 2, 3.1.4, 6
- [55] Y. Song and S. Ermon, "Generative modeling by estimating gradients of the data distribution," *Advances in Neural Information Processing Systems*, vol. 32, 2019. 2.2.2, 3, 4.1.1, 6
- [56] S. Lyu, "Interpretation and generalization of score matching," *arXiv preprint arXiv:1205.2629*, 2012. 2.2.2
- [57] L. Arnold, "Stochastic differential equations," *New York*, 1974. 2.2.2
- [58] B. Oksendal, *Stochastic differential equations: an introduction with applications*. Springer Science & Business Media, 2013. 2.2.2
- [59] D. Watson, J. Ho, M. Norouzi, and W. Chan, "Learning to efficiently sample from diffusion probabilistic models," *arXiv preprint arXiv:2106.03802*, 2021. 2.2.2, 2, 3.1.2, 4
- [60] A. Hyvärinen and P. Dayan, "Estimation of non-normalized statistical models by score matching," *Journal of Machine Learning Research*, vol. 6, no. 4, 2005. 2.2.2
- [61] Y. Song, S. Garg, J. Shi, and S. Ermon, "Sliced score matching: A scalable approach to density and score estimation," in *Uncertainty in Artificial Intelligence*. PMLR, 2020, pp. 574–584. 2.2.2, 6
- [62] D. Maoutsa, S. Reich, and M. Opper, "Interacting particle solutions of fokker-planck equations through gradient-log-density estimation," *Entropy*, vol. 22, no. 8, p. 802, 2020. 2.2.3
- [63] R. T. Chen, Y. Rubanova, J. Bettencourt, and D. K. Duvenaud, "Neural ordinary differential equations," *Advances in neural information processing systems*, vol. 31, 2018. 2.2.3, 3.1.2, 3.1.4
- [64] L. Liu, Y. Ren, Z. Lin, and Z. Zhao, "Pseudo numerical methods for diffusion models on manifolds," *arXiv preprint arXiv:2202.09778*, 2022. 2.2.3, 2, 3.1.2, 3, 3.2.3
- [65] R. W. Hamming, "Stable predictor-corrector methods for ordinary differential equations," *Journal of the ACM (JACM)*, vol. 6, no. 1, pp. 37–47, 1959. 2.4.3
- [66] J. R. Dormand and P. J. Prince, "A family of embedded runge-kutta formulae," *Journal of computational and applied mathematics*, vol. 6, no. 1, pp. 19–26, 1980. 2.4.3
- [67] T. Sauer, *Numerical analysis*. Addison-Wesley Publishing Company, 2011. 2.4.3
- [68] W. H. Press, S. A. Teukolsky, W. T. Vetterling, and B. P. Flannery, *Numerical recipes 3rd edition: The art of scientific computing*. Cambridge university press, 2007. 2.4.3
- [69] A. Borji, "Pros and cons of gan evaluation measures: New developments," *Computer Vision and Image Understanding*, vol. 215, p. 103329, 2022. 2.5.1
- [70] T. Salimans, I. Goodfellow, W. Zaremba, V. Cheung, A. Radford, and X. Chen, "Improved techniques for training gans," *Advances in neural information processing systems*, vol. 29, 2016. 2.5.1
- [71] S. Kullback, *Information theory and statistics*. Courier Corporation, 1997. 2.5.1
- [72] S. Barratt and R. Sharma, "A note on the inception score," 2018. [Online]. Available: <https://arxiv.org/abs/1801.01973> 2.5.2
- [73] M. Heusel, H. Ramsauer, T. Unterthiner, B. Nessler, and S. Hochreiter, "Gans trained by a two time-scale update rule converge to a local nash equilibrium," in *Advances in Neural Information Processing Systems*, I. Guyon, U. V. Luxburg, S. Bengio, H. Wallach, R. Fergus, S. Vishwanathan, and R. Garnett, Eds., vol. 30. Curran Associates, Inc., 2017. [Online]. Available: <https://proceedings.neurips.cc/paper/2017/file/8a1d694707eb0fefe65871369074926d-Paper.pdf> 2.5.2
- [74] A. Razavi, A. Van den Oord, and O. Vinyals, "Generating diverse high-fidelity images with vq-vae-2," *Advances in neural information processing systems*, vol. 32, 2019. 2.5.3
- [75] T. M. Nguyen, A. Garg, R. G. Baraniuk, and A. Anandkumar, "Infocnf: Efficient conditional continuous normalizing flow using adaptive solvers," 2019. 2.5.3
- [76] Z. Ziegler and A. Rush, "Latent normalizing flows for discrete sequences," in *International Conference on Machine Learning*. PMLR, 2019, pp. 7673–7682. 2.5.3
- [77] A. Abdelhamed, M. A. Brubaker, and M. S. Brown, "Noise flow: Noise modeling with conditional normalizing flows," in *Proceedings of the IEEE/CVF International Conference on Computer Vision*, 2019, pp. 3165–3173. 2.5.3
- [78] X. Wei, H. van Gorp, L. Gonzalez-Carabarin, D. Freedman, Y. C. Eldar, and R. J. van Sloun, "Deep unfolding with normalizing flow priors for inverse problems," *IEEE Transactions on Signal Processing*, vol. 70, pp. 2962–2971, 2022. 2.5.3
- [79] B. Máté, S. Klein, T. Golling, and F. Fleuret, "Flowification: Everything is a normalizing flow," *arXiv preprint arXiv:2205.15209*, 2022. 2.5.3
- [80] J. Tomczak and M. Welling, "Vae with a vampprior," in *International Conference on Artificial Intelligence and Statistics*. PMLR, 2018, pp. 1214–1223. 2.5.3
- [81] P. Notin, J. M. Hernández-Lobato, and Y. Gal, "Improving black-box optimization in vae latent space using decoder uncertainty," *Advances in Neural Information Processing Systems*, vol. 34, pp. 802–814, 2021. 2.5.3
- [82] O. Rybkin, K. Daniilidis, and S. Levine, "Simple and effective vae training with calibrated decoders," in *International Conference on Machine Learning*. PMLR, 2021, pp. 9179–9189. 2.5.3
- [83] N. Chen, Y. Zhang, H. Zen, R. J. Weiss, M. Norouzi, and W. Chan, "Wavegrad: Estimating gradients for waveform generation," in *International Conference on Learning Representations*, 2020. 3, 3.1.3, 4.3
- [84] C. Saharia, W. Chan, H. Chang, C. Lee, J. Ho, T. Salimans, D. Fleet, and M. Norouzi, "Palette: Image-to-image diffusion models," in *ACM SIGGRAPH 2022 Conference Proceedings*, 2022, pp. 1–10. 3, 3.1.3, 4.1.1
- [85] E. Luhman and T. Luhman, "Knowledge distillation in iterative generative models for improved sampling speed," *arXiv preprint arXiv:2101.02388*, 2021. 2, 5
- [86] H. Zheng, P. He, W. Chen, and M. Zhou, "Truncated diffusion probabilistic models," *arXiv preprint arXiv:2202.09671*, 2022. 3.1.1, 2, 5, 6
- [87] A. Bansal, E. Borgnia, H.-M. Chu, J. S. Li, H. Kazemi, F. Huang, M. Goldblum, J. Geiping, and T. Goldstein, "Cold diffusion: Inverting arbitrary image transforms without noise," 2022. [Online]. Available: <https://arxiv.org/abs/2208.09392> 3.1.1, 2, 3.1.1
- [88] G. Franzese, S. Rossi, L. Yang, A. Finamore, D. Rossi, M. Filippone, and P. Michiardi, "How much is enough? a study on diffusion times in score-based generative models," 2022. [Online]. Available: <https://arxiv.org/abs/2206.05173> 3.1.1, 2, 5
- [89] Q. Zhang and Y. Chen, "Fast sampling of diffusion models with exponential integrator," *arXiv preprint arXiv:2204.13902*, 2022. 3.1.1, 2, 3.1.2, 3.1.4, 5, 6
- [90] R. San-Roman, E. Nachmani, and L. Wolf, "Noise estimation for generative diffusion models," *arXiv preprint arXiv:2104.02600*, 2021. 3.1.1, 2
- [91] J. Austin, D. D. Johnson, J. Ho, D. Tarlow, and R. van den Berg, "Structured denoising diffusion models in discrete state-spaces," *Advances in Neural Information Processing Systems*, vol. 34, pp. 17981–17993, 2021. 2, 3.1.1, 3.2.2, 6

- [92] F. Bao, C. Li, J. Zhu, and B. Zhang, "Analytic-dpm: an analytic estimate of the optimal reverse variance in diffusion probabilistic models," *arXiv preprint arXiv:2201.06503*, 2022. 2, 3.1.2, 3, 4, 5, 6
- [93] J. Song, C. Meng, and S. Ermon, "Denoising diffusion implicit models," in *International Conference on Learning Representations*, 2020. 3.1.1, 2, 3.1.2, 5
- [94] Q. Zhang, M. Tao, and Y. Chen, "gddim: Generalized denoising diffusion implicit models," *arXiv preprint arXiv:2206.05564*, 2022. 2, 3.1.2, 3.1.4, 5
- [95] D. Kim, B. Na, S. J. Kwon, D. Lee, W. Kang, and I.-C. Moon, "Maximum likelihood training of implicit nonlinear diffusion models," *arXiv preprint arXiv:2205.13699*, 2022. 2, 3.1.2, 6
- [96] A. Jolicœur-Martineau, K. Li, R. Piché-Taillefer, T. Kachman, and I. Mitliagkas, "Gotta go fast when generating data with score-based models," 2021. [Online]. Available: <https://arxiv.org/abs/2105.14080> 2, 3.1.2, 5, 6
- [97] D. Watson, W. Chan, J. Ho, and M. Norouzi, "Learning fast samplers for diffusion models by differentiating through sample quality," 2, 3.1.2, 4, 5
- [98] K. Pandey, A. Mukherjee, P. Rai, and A. Kumar, "Diffusevae: Efficient, controllable and high-fidelity generation from low-dimensional latents," 2022. [Online]. Available: <https://arxiv.org/abs/2201.00308> 2, 3.1.3, 3, 5, 6
- [99] Q. Zhang and Y. Chen, "Diffusion normalizing flow," *Advances in Neural Information Processing Systems*, vol. 34, pp. 16 280–16 291, 2021. 2, 3.1.3, 5
- [100] A. Vahdat, K. Kreis, and J. Kautz, "Score-based generative modeling in latent space," *Advances in Neural Information Processing Systems*, vol. 34, pp. 11 287–11 302, 2021. 2, 3.1.3, 3.1.3, 4.1.2, 5
- [101] Y. Song, C. Durkan, I. Murray, and S. Ermon, "Maximum likelihood training of score-based diffusion models," *Advances in Neural Information Processing Systems*, vol. 34, pp. 1415–1428, 2021. 2, 3.1.3, 3.2.1
- [102] D. Kim, B. Na, S. J. Kwon, D. Lee, W. Kang, and I.-c. Moon, "Maximum likelihood training of parametrized diffusion model," 2021. 2, 3.1.3
- [103] W. Gong and Y. Li, "Interpreting diffusion score matching using normalizing flow," 2021. [Online]. Available: <https://arxiv.org/abs/2107.10072> 2, 3.1.4
- [104] V. De Bortoli, A. Doucet, J. Heng, and J. Thornton, "Simulating diffusion bridges with score matching," 2021. [Online]. Available: <https://arxiv.org/abs/2111.07243> 2, 3.1.4
- [105] L. Zhou, Y. Du, and J. Wu, "3d shape generation and completion through point-voxel diffusion," in *Proceedings of the IEEE/CVF International Conference on Computer Vision (ICCV)*, October 2021, pp. 5826–5835. 2, 3.2.1
- [106] S. Luo and W. Hu, "Diffusion probabilistic models for 3d point cloud generation," in *Proceedings of the IEEE/CVF Conference on Computer Vision and Pattern Recognition*, 2021, pp. 2837–2845. 2, 3.2.1, 3.1.3, 4.1.3
- [107] Z. Lyu, Z. Kong, X. Xu, L. Pan, and D. Lin, "A conditional point diffusion-refinement paradigm for 3d point cloud completion," *arXiv preprint arXiv:2112.03530*, 2021. 2, 3.2.1, 3.1.3, 4.1.3
- [108] A.-C. Cheng, X. Li, S. Liu, M. Sun, and M.-H. Yang, "Autoregressive 3d shape generation via canonical mapping," 2022. [Online]. Available: <https://arxiv.org/abs/2204.01955> 2, 3.2.1
- [109] E. Hoogeboom, D. Nielsen, P. Jaini, P. Forré, and M. Welling, "Argmax flows and multinomial diffusion: Towards non-autoregressive language models," 2021. 2, 3.2.2
- [110] E. Hoogeboom, A. A. Gritsenko, J. Bastings, B. Poole, R. v. d. Berg, and T. Salimans, "Autoregressive diffusion models," *arXiv preprint arXiv:2110.02037*, 2021. 2, 3.2.2
- [111] A. Campbell, J. Benton, V. De Bortoli, T. Rainforth, G. Deligianidis, and A. Doucet, "A continuous time framework for discrete denoising models," *arXiv preprint arXiv:2205.14987*, 2022. 2, 3.2.2
- [112] S. Gu, D. Chen, J. Bao, F. Wen, B. Zhang, D. Chen, L. Yuan, and B. Guo, "Vector quantized diffusion model for text-to-image synthesis," in *Proceedings of the IEEE/CVF Conference on Computer Vision and Pattern Recognition*, 2022, pp. 10 696–10 706. 2, 3.2.2
- [113] Z. Tang, S. Gu, J. Bao, D. Chen, and F. Wen, "Improved vector quantized diffusion models," *arXiv preprint arXiv:2205.16007*, 2022. 2, 3.2.2
- [114] M. Cohen, G. Quispe, S. L. Corff, C. Ollion, and E. Moulines, "Diffusion bridges vector quantized variational autoencoders," 2022. [Online]. Available: <https://arxiv.org/abs/2202.04895> 2, 3.2.2
- [115] P. Xie, Q. Zhang, Z. Li, H. Tang, Y. Du, and X. Hu, "Vector quantized diffusion model with codeunet for text-to-sign pose sequences generation," 2022. [Online]. Available: <https://arxiv.org/abs/2208.09141> 2, 3.2.2
- [116] V. De Bortoli, E. Mathieu, M. Hutchinson, J. Thornton, Y. W. Teh, and A. Doucet, "Riemannian score-based generative modeling," *arXiv preprint arXiv:2202.02763*, 2022. 2, 3.2.3
- [117] C.-W. Huang, M. Aghajohari, A. J. Bose, P. Panangaden, and A. Courville, "Riemannian diffusion models," *arXiv preprint arXiv:2208.07949*, 2022. 2, 3.2.3
- [118] C. Niu, Y. Song, J. Song, S. Zhao, A. Grover, and S. Ermon, "Permutation invariant graph generation via score-based generative modeling," in *International Conference on Artificial Intelligence and Statistics*. PMLR, 2020, pp. 4474–4484. 2, 3.2.3
- [119] J. Gou, B. Yu, S. J. Maybank, and D. Tao, "Knowledge distillation: A survey," *International Journal of Computer Vision*, vol. 129, no. 6, pp. 1789–1819, 2021. 3.1.1
- [120] R. Huang, Z. Zhao, H. Liu, J. Liu, C. Cui, and Y. Ren, "Prodiff: Progressive fast diffusion model for high-quality text-to-speech," 2022. [Online]. Available: <https://arxiv.org/abs/2207.06389> 3.1.1
- [121] A. M. Mood, "Introduction to the theory of statistics." 1950. 3.1.1
- [122] H. Zheng and M. Zhou, "Act: Asymptotic conditional transport," 2020. 3.1.1
- [123] S. Mohamed and B. Lakshminarayanan, "Learning in implicit generative models," *Learning*, no. 1/14, 2018. 3.1.2
- [124] W. Grathwohl, R. T. Chen, J. Bettencourt, I. Sutskever, and D. Duvenaud, "Ffjord: Free-form continuous dynamics for scalable reversible generative models," *arXiv preprint arXiv:1810.01367*, 2018. 3.1.2, 3.1.4
- [125] T. Dockhorn, A. Vahdat, and K. Kreis, "Score-based generative modeling with critically-damped langevin diffusion," *arXiv preprint arXiv:2112.07068*, 2021. 3.1.2
- [126] M. Bayram, T. Partal, and G. Orucova Buyukoz, "Numerical methods for simulation of stochastic differential equations," *Advances in Difference Equations*, vol. 2018, no. 1, pp. 1–10, 2018. 3.1.2
- [127] V. F. Zaitsev and A. D. Polyanin, *Handbook of exact solutions for ordinary differential equations*. CRC press, 2002. 3.1.2
- [128] J. C. Butcher, *Numerical methods for ordinary differential equations*. John Wiley & Sons, 2016. 3.1.2
- [129] G. N. Milstein, *Numerical integration of stochastic differential equations*. Springer Science & Business Media, 1994, vol. 313. 3.1.2
- [130] E. Platen and N. Bruti-Liberati, *Numerical solution of stochastic differential equations with jumps in finance*. Springer Science & Business Media, 2010, vol. 64. 3.1.2
- [131] E. Süli and D. F. Mayers, *An introduction to numerical analysis*. Cambridge university press, 2003. 3.1.2
- [132] F. Rabiei, F. Ismail, and M. Suleiman, "Improved runge-kutta methods for solving ordinary differential equations," *Sains Malaysiana*, vol. 42, no. 11, pp. 1679–1687, 2013. 3.1.2
- [133] C. W. Gear and D. R. Wells, "Multirate linear multistep methods," *BIT Numerical Mathematics*, vol. 24, no. 4, pp. 484–502, 1984. 3.1.2
- [134] L. F. Shampine, *Numerical solution of ordinary differential equations*. Routledge, 2018. 3.1.2
- [135] Q. Han and S. Ji, "Novel multi-step predictor-corrector schemes for backward stochastic differential equations," 2021. [Online]. Available: <https://arxiv.org/abs/2102.05915> 3.1.2
- [136] M. Hochbruck and A. Ostermann, "Exponential integrators," *Acta Numerica*, vol. 19, pp. 209–286, 2010. 3.1.2
- [137] T. H. Cormen, C. E. Leiserson, R. L. Rivest, and C. Stein, *Introduction to algorithms*. MIT press, 2022. 3.1.2
- [138] D. Watson, W. Chan, J. Ho, and M. Norouzi, "Learning fast samplers for diffusion models by differentiating through sample quality," in *International Conference on Learning Representations*, 2021. 3.1.2
- [139] R. Kumar, M. Purohit, Z. Svitkina, E. Vee, and J. Wang, "Efficient rematerialization for deep networks," *Advances in Neural Information Processing Systems*, vol. 32, 2019. 3.1.2
- [140] J. Ho, X. Chen, A. Srinivas, Y. Duan, and P. Abbeel, "Flow++: Improving flow-based generative models with variational dequantization and architecture design," in *Proceedings of the 36th International Conference on Machine Learning*, ser. Proceedings of Machine Learning Research, K. Chaudhuri and R. Salakhutdinov, Eds., vol. 97. PMLR, 09–15 Jun 2019, pp. 2722–2730. [Online]. Available: <https://proceedings.mlr.press/v97/ho19a.html> 3.1.3, 3.2.1

- [141] E. Hoogeboom, T. S. Cohen, and J. M. Tomczak, "Learning discrete distributions by dequantization," *arXiv preprint arXiv:2001.11235*, 2020. 3.1.3, 3.2.1
- [142] B. Uria, I. Murray, and H. Larochelle, "Rnade: The real-valued neural autoregressive density-estimator," *Advances in Neural Information Processing Systems*, vol. 26, 2013. 3.1.3, 3.2.1
- [143] L. Theis, A. van den Oord, and M. Bethge, "A note on the evaluation of generative models," in *International Conference on Learning Representations (ICLR 2016)*, 2016, pp. 1–10. 3.1.3, 3.2.1
- [144] D. Kim, S. Shin, K. Song, W. Kang, and I.-C. Moon, "Soft truncation: A universal training technique of score-based diffusion model for high precision score estimation," 2021. [Online]. Available: <https://arxiv.org/abs/2106.05527> 3, 6
- [145] H. Chung, B. Sim, D. Ryu, and J. C. Ye, "Improving diffusion models for inverse problems using manifold constraints," *arXiv preprint arXiv:2206.00941*, 2022. 4
- [146] G. Batzolis, J. Stanczuk, C.-B. Schönlieb, and C. Etmann, "Conditional image generation with score-based diffusion models," *arXiv preprint arXiv:2111.13606*, 2021. 3.1.3, 4.1.1
- [147] B. Kawar, M. Elad, S. Ermon, and J. Song, "Denoising diffusion restoration models," in *ICLR Workshop on Deep Generative Models for Highly Structured Data*, 2022. 3.1.3, 4.1.1
- [148] L. Theis, T. Salimans, M. D. Hoffman, and F. Mentzer, "Lossy compression with gaussian diffusion," *arXiv preprint arXiv:2206.08889*, 2022. 3.1.3, 4.1.1
- [149] H. Li, Y. Yang, M. Chang, S. Chen, H. Feng, Z. Xu, Q. Li, and Y. Chen, "Srdiff: Single image super-resolution with diffusion probabilistic models," *Neurocomputing*, vol. 479, pp. 47–59, 2022. 3.1.3, 4.1.1
- [150] A. Lugmayr, M. Danelljan, A. Romero, F. Yu, R. Timofte, and L. Van Gool, "Repaint: Inpainting using denoising diffusion probabilistic models," in *Proceedings of the IEEE/CVF Conference on Computer Vision and Pattern Recognition*, 2022, pp. 11 461–11 471. 3.1.3, 4.1.1
- [151] G. Giannone, D. Nielsen, and O. Winther, "Few-shot diffusion models," *arXiv preprint arXiv:2205.15463*, 2022. 3.1.3, 4.1.2
- [152] X. Han, H. Zheng, and M. Zhou, "Card: Classification and regression diffusion models," *arXiv preprint arXiv:2206.07275*, 2022. 3.1.3, 4.1.2
- [153] A. Nichol, P. Dhariwal, A. Ramesh, P. Shyam, P. Mishkin, B. McGrew, I. Sutskever, and M. Chen, "Glide: Towards photorealistic image generation and editing with text-guided diffusion models," *arXiv preprint arXiv:2112.10741*, 2021. 3.1.3, 4.1.2
- [154] T. Amit, E. Nachmani, T. Shaharabany, and L. Wolf, "Segdiff: Image segmentation with diffusion probabilistic models," *arXiv preprint arXiv:2112.00390*, 2021. 3.1.3, 4.1.2
- [155] R. Huang, Z. Zhao, H. Liu, J. Liu, C. Cui, and Y. Ren, "Prodiff: Progressive fast diffusion model for high-quality text-to-speech," *arXiv preprint arXiv:2207.06389*, 2022. 3.1.3, 4.1.2, 4.3
- [156] L. Zhou, Y. Du, and J. Wu, "3d shape generation and completion through point-voxel diffusion," in *Proceedings of the IEEE/CVF International Conference on Computer Vision*, 2021, pp. 5826–5835. 3.1.3, 4.1.3
- [157] S. Luo and W. Hu, "Score-based point cloud denoising," in *Proceedings of the IEEE/CVF International Conference on Computer Vision*, 2021, pp. 4583–4592. 3.1.3, 4.1.3
- [158] R. Yang, P. Srivastava, and S. Mandt, "Diffusion probabilistic modeling for video generation," *arXiv preprint arXiv:2203.09481*, 2022. 3.1.3, 4.1.4
- [159] W. Harvey, S. Naderiparizi, V. Masrani, C. Weilbach, and F. Wood, "Flexible diffusion modeling of long videos," *arXiv preprint arXiv:2205.11495*, 2022. 3.1.3, 4.1.4
- [160] V. Voleti, A. Jolicœur-Martineau, and C. Pal, "Mcvd: Masked conditional video diffusion for prediction, generation, and interpolation," *arXiv preprint arXiv:2205.09853*, 2022. 3.1.3, 4.1.4
- [161] T. Höpfe, A. Mehrjou, S. Bauer, D. Nielsen, and A. Dittadi, "Diffusion models for video prediction and infilling," *arXiv preprint arXiv:2206.07696*, 2022. 3.1.3, 4.1.4
- [162] H. Chung and J. C. Ye, "Score-based diffusion models for accelerated mri," *Medical Image Analysis*, p. 102479, 2022. 3.1.3, 4.1.5
- [163] Y. Song, L. Shen, L. Xing, and S. Ermon, "Solving inverse problems in medical imaging with score-based generative models," in *International Conference on Learning Representations*, 2021. 3.1.3, 4.1.5
- [164] H. Chung, E. S. Lee, and J. C. Ye, "Mr image denoising and super-resolution using regularized reverse diffusion," *arXiv preprint arXiv:2203.12621*, 2022. 3.1.3, 4.1.5
- [165] X. L. Li, J. Thickstun, I. Gulrajani, P. Liang, and T. B. Hashimoto, "Diffusion-lm improves controllable text generation," *arXiv preprint arXiv:2205.14217*, 2022. 3.1.3, 4.2.1
- [166] T. Chen, R. Zhang, and G. Hinton, "Analog bits: Generating discrete data using diffusion models with self-conditioning," *arXiv preprint arXiv:2208.04202*, 2022. 3.1.3, 4.2.1
- [167] Y. Tashiro, J. Song, Y. Song, and S. Ermon, "Csd: Conditional score-based diffusion models for probabilistic time series imputation," *Advances in Neural Information Processing Systems*, vol. 34, pp. 24 804–24 816, 2021. 3.1.3, 4.2.2
- [168] J. M. L. Alcaraz and N. Strodthoff, "Diffusion-based time series imputation and forecasting with structured state space models," *arXiv preprint arXiv:2208.09399*, 2022. 3.1.3, 4.2.2
- [169] S. W. Park, K. Lee, and J. Kwon, "Neural markov controlled sde: Stochastic optimization for continuous-time data," in *International Conference on Learning Representations*, 2021. 3.1.3, 4.2.2
- [170] Z. Kong, W. Ping, J. Huang, K. Zhao, and B. Catanzaro, "Diffwave: A versatile diffusion model for audio synthesis," in *International Conference on Learning Representations*, 2020. 3.1.3, 4.3
- [171] V. Popov, I. Vovk, V. Gogoryan, T. Sadekova, and M. Kudinov, "Grad-tts: A diffusion probabilistic model for text-to-speech," in *International Conference on Machine Learning*. PMLR, 2021, pp. 8599–8608. 3.1.3, 4.3
- [172] M. Jeong, H. Kim, S. J. Cheon, B. J. Choi, and N. S. Kim, "Diff-TTS: A Denoising Diffusion Model for Text-to-Speech," in *Proc. Interspeech 2021*, 2021, pp. 3605–3609. 3.1.3, 4.3
- [173] V. Popov, I. Vovk, V. Gogoryan, T. Sadekova, M. S. Kudinov, and J. Wei, "Diffusion-based voice conversion with fast maximum likelihood sampling scheme," in *International Conference on Learning Representations*, 2021. 3.1.3, 4.3
- [174] J. Liu, C. Li, Y. Ren, F. Chen, and Z. Zhao, "Diffsinger: Singing voice synthesis via shallow diffusion mechanism," in *Proceedings of the AAAI Conference on Artificial Intelligence*, vol. 36, no. 10, 2022, pp. 11 020–11 028. 3.1.3, 4.3
- [175] D. Yang, J. Yu, H. Wang, W. Wang, C. Weng, Y. Zou, and D. Yu, "Diffsound: Discrete diffusion model for text-to-sound generation," *arXiv preprint arXiv:2207.09983*, 2022. 3.1.3, 4.3
- [176] J. Tae, H. Kim, and T. Kim, "Editts: Score-based editing for controllable text-to-speech," *arXiv preprint arXiv:2110.02584*, 2021. 3.1.3, 4.3
- [177] H. Kim, S. Kim, and S. Yoon, "Guided-tts: A diffusion model for text-to-speech via classifier guidance," in *International Conference on Machine Learning*. PMLR, 2022, pp. 11 119–11 133. 3.2, 3.1.3, 4.3
- [178] S. Kim, H. Kim, and S. Yoon, "Guided-tts 2: A diffusion model for high-quality adaptive text-to-speech with untranscribed data," *arXiv preprint arXiv:2205.15370*, 2022. 3.1.3, 4.3
- [179] A. Levkovitch, E. Nachmani, and L. Wolf, "Zero-shot voice conditioning for denoising diffusion tts models," *arXiv preprint arXiv:2206.02246*, 2022. 3.1.3, 4.3
- [180] Y. Koizumi, H. Zen, K. Yatabe, N. Chen, and M. Bacchiani, "Specgrad: Diffusion probabilistic model based neural vocoder with adaptive noise spectral shaping," *arXiv preprint arXiv:2203.16749*, 2022. 3.1.3, 4.3
- [181] Y. Leng, Z. Chen, J. Guo, H. Liu, J. Chen, X. Tan, D. Mandic, L. He, X.-Y. Li, T. Qin *et al.*, "Binauralgrad: A two-stage conditional diffusion probabilistic model for binaural audio synthesis," *arXiv preprint arXiv:2205.14807*, 2022. 3.1.3, 4.3
- [182] C. Shi, S. Luo, M. Xu, and J. Tang, "Learning gradient fields for molecular conformation generation," in *International Conference on Machine Learning*. PMLR, 2021, pp. 9558–9568. 3.1.3, 4.4.1
- [183] S. Luo, C. Shi, M. Xu, and J. Tang, "Predicting molecular conformation via dynamic graph score matching," *Advances in Neural Information Processing Systems*, vol. 34, pp. 19 784–19 795, 2021. 3.1.3, 4.4.1
- [184] B. Jing, G. Corso, R. Barzilay, and T. S. Jaakkola, "Torsional diffusion for molecular conformer generation," in *ICLR2022 Machine Learning for Drug Discovery*, 2022. 3.2, 3.1.3, 4.4.1
- [185] T. Xie, X. Fu, O.-E. Ganea, R. Barzilay, and T. S. Jaakkola, "Crystal diffusion variational autoencoder for periodic material generation," in *International Conference on Learning Representations*, 2021. 3.1.3, 4.4.2
- [186] S. Luo, Y. Su, X. Peng, S. Wang, J. Peng, and J. Ma, "Antigen-specific antibody design and optimization with diffusion-based generative models," *bioRxiv*, 2022. 3.2, 3.1.3, 4.4.2

- [187] N. Anand and T. Achim, "Protein structure and sequence generation with equivariant denoising diffusion probabilistic models," *arXiv preprint arXiv:2205.15019*, 2022. 3.1.3, 4.4.2
- [188] J. S. Lee and P. M. Kim, "Proteinsgm: Score-based generative modeling for de novo protein design," *bioRxiv*, 2022. 3.1.3, 4.4.2
- [189] L. Alili, P. Graczyk, and T. Zak, "On inversions and doob h-transforms of linear diffusions," *Lecture Notes in Mathematics*, vol. 2137, 09 2012. 3.1.4
- [190] A. Van Den Oord, O. Vinyals *et al.*, "Neural discrete representation learning," *Advances in neural information processing systems*, vol. 30, 2017. 3.2.2
- [191] H. A. Pierson and M. S. Gashler, "Deep learning in robotics: a review of recent research," *Advanced Robotics*, vol. 31, no. 16, pp. 821–835, 2017. 3.2.3
- [192] N. Sünderhauf, O. Brock, W. Scheirer, R. Hadsell, D. Fox, J. Leitner, B. Upcroft, P. Abbeel, W. Burgard, M. Milford *et al.*, "The limits and potentials of deep learning for robotics," *The International journal of robotics research*, vol. 37, no. 4-5, pp. 405–420, 2018. 3.2.3
- [193] R. P. De Lima, K. Marfurt, D. Duarte, and A. Bonar, "Progress and challenges in deep learning analysis of geoscience images," in *81st EAGE Conference and Exhibition 2019*, vol. 2019, no. 1. European Association of Geoscientists & Engineers, 2019, pp. 1–5. 3.2.3
- [194] L. Zhang, L. Zhang, and B. Du, "Deep learning for remote sensing data: A technical tutorial on the state of the art," *IEEE Geoscience and remote sensing magazine*, vol. 4, no. 2, pp. 22–40, 2016. 3.2.3
- [195] M. Reichstein, G. Camps-Valls, B. Stevens, M. Jung, J. Denzler, N. Carvalhais *et al.*, "Deep learning and process understanding for data-driven earth system science," *Nature*, vol. 566, no. 7743, pp. 195–204, 2019. 3.2.3
- [196] J. Wang, H. Cao, J. Z. Zhang, and Y. Qi, "Computational protein design with deep learning neural networks," *Scientific reports*, vol. 8, no. 1, pp. 1–9, 2018. 3.2.3
- [197] W. Cao, Z. Yan, Z. He, and Z. He, "A comprehensive survey on geometric deep learning," *IEEE Access*, vol. 8, pp. 35 929–35 949, 2020. 3.2.3
- [198] J. M. Lee, "Smooth manifolds," in *Introduction to smooth manifolds*. Springer, 2013, pp. 1–31. 3.2.3
- [199] —, *Introduction to Riemannian manifolds*. Springer, 2018, vol. 176. 3.2.3
- [200] G. Leobacher and A. Steinicke, "Existence, uniqueness and regularity of the projection onto differentiable manifolds," *Annals of global analysis and geometry*, vol. 60, no. 3, pp. 559–587, 2021. 3.2.3
- [201] G. Wanner and E. Hairer, *Solving ordinary differential equations II*. Springer Berlin Heidelberg New York, 1996, vol. 375. 3.2.3
- [202] L. Wu, H. Lin, Z. Gao, C. Tan, and S. Z. Li, "Self-supervised on graphs: Contrastive, generative, or predictive," 2021. 3.2.3
- [203] A. Krizhevsky, G. Hinton *et al.*, "Learning multiple layers of features from tiny images," 2009. 3.3
- [204] A. Krizhevsky, I. Sutskever, and G. E. Hinton, "Imagenet classification with deep convolutional neural networks," *Communications of the ACM*, vol. 60, no. 6, pp. 84–90, 2017. 3.3
- [205] Z. Liu, P. Luo, X. Wang, and X. Tang, "Deep learning face attributes in the wild," in *Proceedings of International Conference on Computer Vision (ICCV)*, December 2015. 3.3
- [206] F. Yu, A. Seff, Y. Zhang, S. Song, T. Funkhouser, and J. Xiao, "Lsun: Construction of a large-scale image dataset using deep learning with humans in the loop," *arXiv preprint arXiv:1506.03365*, 2015. 3.3
- [207] T. Karras, S. Laine, and T. Aila, "A style-based generator architecture for generative adversarial networks," in *Proceedings of the IEEE/CVF Conference on Computer Vision and Pattern Recognition (CVPR)*, June 2019. 3.3
- [208] Y. LeCun and C. Cortes, "MNIST handwritten digit database," 2010. [Online]. Available: <http://yann.lecun.com/exdb/mnist/> 3.3
- [209] A. Radford, J. W. Kim, C. Hallacy, A. Ramesh, G. Goh, S. Agarwal, G. Sastry, A. Askell, P. Mishkin, J. Clark *et al.*, "Learning transferable visual models from natural language supervision," in *International Conference on Machine Learning*. PMLR, 2021, pp. 8748–8763. 4.1.2
- [210] T.-Y. Lin, M. Maire, S. Belongie, J. Hays, P. Perona, D. Ramanan, P. Dollár, and C. L. Zitnick, "Microsoft coco: Common objects in context," in *European conference on computer vision*. Springer, 2014, pp. 740–755. 4.1.2
- [211] Z. Chen, X. Tan, K. Wang, S. Pan, D. Mandic, L. He, and S. Zhao, "Infergrad: Improving diffusion models for vocoder by considering inference in training," in *ICASSP 2022-2022 IEEE International Conference on Acoustics, Speech and Signal Processing (ICASSP)*. IEEE, 2022, pp. 8432–8436. 4.3
- [212] W. Jin, J. Wohlwend, R. Barzilay, and T. S. Jaakkola, "Iterative refinement graph neural network for antibody sequence-structure co-design," in *International Conference on Learning Representations*, 2021. 4.4.2
- [213] T. Fu and J. Sun, "Antibody complementarity determining regions (cdrs) design using constrained energy model," in *Proceedings of the 28th ACM SIGKDD Conference on Knowledge Discovery and Data Mining*, 2022, pp. 389–399. 4.4.2
- [214] W. Jin, R. Barzilay, and T. Jaakkola, "Antibody-antigen docking and design via hierarchical structure refinement," in *International Conference on Machine Learning*. PMLR, 2022, pp. 10 217–10 227. 4.4.2
- [215] Y. Song and S. Ermon, "Improved techniques for training score-based generative models," *Advances in neural information processing systems*, vol. 33, pp. 12 438–12 448, 2020. 6

APPENDIX A BENCHMARKS ON CIFAR-10 DATASET

TABLE 5
Benchmarks on CIFAR-10 (NFE < 1000)

Method	NFE	FID	IS	NLL
Diffusion Step [88]	600	3.72	-	-
ES-DDPM [51]	600	3.17	-	-
Diffusion Step [88]	400	14.38	-	-
Diffusion Step [88]	200	5.44	-	-
Gotta Go Fast VP [89]	180	2.44	-	-
Gotta Go Fast VE [89]	180	3.40	-	-
Gotta Go Fast VP [89]	148	2.73	-	-
Gotta Go Fast VE [89]	148	10.15	-	-
LSGM [100]	138	2.10	-	-
DDIM [93]	100	4.16	-	-
FastDPM [89]	100	2.86	-	-
TDPM [86]	100	3.10	9.34	-
DiffuseVAE [98]	100	11.71	8.27	-
DiffFlow [99]	100	14.14	-	3.04
Analytic DPM [92]	100	-	-	3.59
Efficient Sampling [96]	64	3.08	-	-
DPM-Solver [50]	51	2.59	-	-
DDIM [93]	50	4.67	-	-
FastDPM [89]	50	3.2	-	-
Improved DDPM [47]	50	4.99	-	-
TDPM [86]	50	3.3	9.22	-
DEIS [96]	50	2.57	-	-
gDDIM [94]	50	2.28	-	-
DPM-Solver Discrete [50]	44	3.48	-	-
Efficient Sampling [96]	32	3.17	-	-
Improved DDPM [47]	25	7.53	-	-
GGDM [97]	25	4.25	9.19	-
DDIM [93]	20	6.84	-	-
FastDPM [89]	20	5.05	-	-
DEIS [96]	20	2.86	-	-
DPM-Solver [50]	20	2.87	-	-
DPM-Solver Discrete [50]	20	3.72	-	-
Efficient Sampling [96]	16	3.41	-	-
DDIM [93]	10	13.36	-	-
FastDPM [89]	10	9.90	-	-
GGDM [97]	10	8.23	8.90	-
Analytic DPM [92]	10	-	-	4.11
DEIS [96]	10	4.17	-	-
DPM-Solver [50]	10	6.96	-	-
DPM-Solver Discrete [50]	10	10.16	-	-
Progressive Distillation [48]	8	2.57	-	-
Denosing Diffusion GAN [49]	8	4.36	9.43	-
GGDM [97]	5	13.77	8.53	-
DEIS [96]	5	15.37	-	-
Progressive Distillation [48]	4	3.00	-	-
TDPM [86]	4	3.41	9.00	-
Denosing Diffusion GAN [49]	4	3.75	9.63	-
Progressive Distillation [48]	2	4.51	-	-
TDPM [86]	2	4.47	8.97	-
Denosing Diffusion GAN [49]	2	4.08	9.80	-
Denosing student [85]	1	9.36	8.36	-
Progressive Distillation [48]	1	9.12	-	-
TDPM [86]	1	8.91	8.65	-

TABLE 6
Benchmarks on CIFAR-10 (NFE ≥ 1000)

Method	NFE	FID	IS	NLL
Improved DDPM [47]	4000	2.90	-	-
VE SDE [53]	2000	2.20	9.89	-
VP SDE [53]	2000	2.41	9.68	3.13
sub-VP SDE [53]	2000	2.41	9.57	2.92
DDPM [52]	1000	3.17	9.46	3.72
NCSN [55]	1000	25.32	8.87	-
SSM [61]	1000	54.33	-	-
NCSNv2 [215]	1000	10.87	8.40	-
D3PM [91]	1000	7.34	8.56	3.44
Efficient Sampling [96]	1000	2.94	-	-
NCSN++ [144]	1000	2.33	10.11	3.04
DDPM++ [144]	1000	2.47	9.78	2.91
TDPM [86]	1000	3.07	9.24	-
VDM [54]	1000	4.00	-	-
DiffuseVAE [98]	1000	8.72	8.63	-
Analytic DPM [92]	1000	-	-	3.59
Gotta Go Fast VP [89]	1000	2.49	-	-
Gotta Go Fast VE [89]	1000	3.14	-	-
INDM [95]	1000	2.28	-	3.09